



**Kaunas University of Technology**  
Faculty of Mechanical Engineering and Design

# **Investigation of Compliant Pressure Actuated Monolithic Joint Design Characteristics**

Master's Final Degree Project

---

**Marius Vaitkevičius**

Project author

**Prof. dr. Alvydas Kondratas**

Supervisor

---

**Kaunas, 2019**



**Kaunas University of Technology**  
Faculty of Mechanical Engineering and Design

# **Investigation of Compliant Pressure Actuated Monolithic Joint Design Characteristics**

Master's Final Degree Project  
Mechatronics (6211EX017)

---

**Marius Vaitkevičius**

Project author

**Prof. dr. Alvydas Kondratas**

Supervisor

**Doc. dr. Inga Skiedraitė**

Reviewer

---

**Kaunas, 2019**



**Kaunas University of Technology**

Faculty of Mechanical Engineering and Design

Marius Vaitkevičius

## **Investigation of Compliant Pressure Actuated Monolithic Joint Design Characteristics**

### **Declaration of Academic Integrity**

I confirm that the final project of mine, Marius Vaitkevičius, on the topic „Investigation of Compliant Pressure Actuated Monolithic Joint Design Characteristics“ is written completely by myself; all the provided data and research results are correct and have been obtained honestly. None of the parts of this thesis have been plagiarised from any printed, Internet-based or otherwise recorded sources. All direct and indirect quotations from external resources are indicated in the list of references. No monetary funds (unless required by Law) have been paid to anyone for any contribution to this project.

I fully and completely understand that any discovery of any manifestations/case/facts of dishonesty inevitably results in me incurring a penalty according to the procedure(s) effective at Kaunas University of Technology.

---

(name and surname filled in by hand)

---

(signature)



**Kaunas University of Technology**

Faculty of Mechanical Engineering and Design

## **Task of the Master's final degree project**

**Given to the student** – Marius Vaitkevičius

### **1. Title of the project –**

Investigation of Compliant Pressure Actuated Monolithic Joint Design Characteristics

*(In English)*

Lankstaus slėgiu varomo monolitinio šarnyro konstrukcijos charakteristikų tyrimas

*(In Lithuanian)*

### **2. Aim and tasks of the project –**

Investigate the viability of a monolithic, actuated joint and compile a set of design notes describing the influence of geometry and material over the performance of said joint.

1. Model a set of overall design variations and test the variations using finite element analysis, determining the most promising design.
2. Refine the most optimal design variation keeping note of geometry-performance correlations.
3. Propose methods of control, propulsion and possible application for the developed joint.

### **3. Initial data of the project –**

Not available

### **4. Main requirements and conditions –**

The actuating and compliant elements of the joint must be integrated in a single, monolithic unit. The joint must display: a substantial range of motion; weight to force ratio comparable to conventional pressure actuated products; relatively high rigidity in directions not related to actuations. A single finite element analysis software and a consistent methodology must be used for all tests to ensure comparable results.

Project author

*(Name, Surname)*

*(Signature)*

*(Date)*

Supervisor

*(Name, Surname)*

*(Signature)*

*(Date)*

Head of study  
field programs

*(Name, Surname)*

*(Signature)*

*(Date)*

Marius Vaitkevičius. Investigation of Compliant Pressure Actuated Monolithic Joint Design Characteristics. Master's Final Degree Project, supervisor Prof. dr. Alvydas Kondratas; Faculty of Mechanical Engineering and Design, Kaunas University of Technology.

Study field and area (study field group): Production and Manufacturing Engineering (E10), Engineering Sciences (E).

Keywords: compliant, monolithic, pressure actuated, additive manufacturing, inflatable, finite element analysis, geometry-performance correlation, comparative study.

Kaunas, 2019. 68 p.

### **Summary**

This study proposes a possibility of producing a fully functional mechanism (comprised of rigid elements, joints and means of propulsion) by a single operation of additive manufacturing. This idea is then reduced to its most basic form – a single actuated, monolithic joint connecting two rigid elements. If such joint is proven viable in terms of performance and ability to adjust performance by design, then the hypothesis of single operation mechanism production would be considered proven.

Study is comprised off four parts:

1. Overview of technologies related to compliant and pressure actuated designs;
2. Establishing basic designs based on information found in part one and determining the most potent one of them;
3. Investigating the correlation between joint geometry and joint performance thus establishing design approach;
4. Providing suggestions for the new joint integration into existing technologies and vice versa.

It was determined that a compliant joint and inflatable bellow combination was the most effective of the basic designs. Upon further investigation of this design, geometry correlations to performance were established. Inflating bellow thickness and bellow profile length were most responsive, compliant element thickness provided minor adjustments and the perimeter on the bellow was proven relatively inert. Knowing this, a preliminary design, modeled for specific application, could be quickly optimized without extensive testing. It was suggested that any method of applying pressure should be able to power the joint, including different types of fluid flow and even thermal expansion. A compact motion tracking solution was necessary and Hall sensor was accepted as most fitting.

Vaitkevičius, Marius. Lankstaus slėgiu varomo monolitinio šarnyro konstrukcijos charakteristikų tyrimas. Magistro baigiamasis projektas, vadovas Prof. dr. Alvydas Kondratas; Kauno technologijos universitetas, Mechanikos inžinerijos ir dizaino fakultetas.

Studijų kryptis ir sritis (studijų krypčių grupė): Gamybos inžinerija (E10), Inžinerijos mokslai (E).

Reikšminiai žodžiai: lankstus, monolitinis, slėgiu varomas, pridėtinė gamyba, pripučiamas, baigtinių elementų metodas, geometrijos-charakteristikos koreliacija, lyginamasis tyrimas.

Kaunas, 2019. 68 p.

### **Santrauka**

Šiame darbe nagrinėjama galimybė gaminti funkcionuojančius mechanizmus viena, pridėtinės gamybos, operacija. Šiuo atveju funkcionuojančiu mechanizmu laikoma konstrukcija, susidedanti iš standžių elementų, šarnyrų ir varomosios jėgos šaltinių. Ši koncepcija supaprastinta iki esminio komponento – vieno varomo, monolitinio šarnyro, jungiančio du standžius elementus. Jei tokio šarnyro darbinės charakteristikos būtų praktiškai pritaikomos ir efektyviai keičiamos kintant geometriniams parametrams, tada hipotezė siūlanti viena operacija gaminamus mechanizmus būtų įrodyta.

Tyrimas susideda iš keturių dalių:

1. Esamų technologijų, susijusių su lanksčiomis ir slėgiu varomomis konstrukcijomis, apžvalga;
2. Paprastų konstrukcijų sukūrimas, remiantis technologijų apžvalgoje gauta informacija ir efektyviausios konstrukcijos atranka;
3. Koreliacijos tarp šarnyro geometrijos ir darbinių charakteristikų tyrimas, sistematizuojama konstravimo metodika;
4. Pasiūlymai naujų šarnyrų integravimo į esamas technologijas ir atvirkščiai klausimu.

Nustatyta, kad lankstaus šarnyro ir pripučiamų dumplių konstrukcija yra efektyviausia iš paprastųjų konstrukcijų. Detalesniu tyrimu buvo nustatytos koreliacijos tarp šios konstrukcijos geometrijos ir darbinių charakteristikų. Pripučiamų dumplių sienelės storis ir dumplių profilio ilgis turėjo didžiausią įtaką darbinėms charakteristikoms. Lankstaus elemento storis sukėlė minimalius pakitimus, o dumplių perimetras įtakos beveik neturėjo. Tai žinant, preliminari konstrukcija, sumodeliuota konkrečiam pritaikymui, būtų optimizuojama išvengiant kruopštaus testavimo. Buvo siūloma, kad bet kuris slėgio taikymo metodas turėtų tikti šarnyro varymui, įskaitant įvairius fluidus ir net terminį plėtimąsi. Siekiant kompaktiško judesio sekimo sprendimo, Holo jutiklis buvo laikomas labiausiai tinkamu.

## Table of contents

<b>List of figures</b> .....	<b>8</b>
<b>List of tables</b> .....	<b>10</b>
<b>Introduction</b> .....	<b>11</b>
<b>1. State-of-the-art overview</b> .....	<b>12</b>
1.1. Compliant mechanisms .....	12
1.1.1. Implications of compliant mechanisms .....	13
1.1.2. Calculation of compliant mechanisms .....	14
1.1.3. Underactuation of compliant mechanisms .....	14
1.2. Inflatable actuators .....	15
1.3. Additively manufactured compliant actuators .....	16
1.4. State-of-the-art overview summary .....	17
<b>2. Design testing</b> .....	<b>18</b>
2.1. Method and equipment .....	18
2.2. Geometrical basis design .....	21
2.2.1. Eccentric thickness design (design 1) .....	21
2.2.2. Corrugated design (design 2) .....	22
2.2.3. Bellow design (design 3) .....	22
<b>3. Results</b> .....	<b>24</b>
3.1. Design 1 TangoBlack .....	24
3.2. Design 1 TPU .....	25
3.3. Design 2 TPU .....	27
3.4. Design 3 TPU .....	29
3.5. Overall design study results .....	31
<b>4. Investigation of design geometry</b> .....	<b>32</b>
4.1. Testing process .....	32
4.2. Baseline model (variation 1111) .....	33
4.3. Alteration of inflatable bladder thickness (group X111) .....	35
4.4. Alteration of pseudo-rigid block area affected by pressure (group 1X11) .....	36
4.5. Alteration of compliant element thickness (group 11X1) .....	38
4.6. Alteration of inflatable bladder material excess (group 111X) .....	40
4.7. Evaluation of geometric elements and design optimization .....	42
<b>5. Joint powering, control and application recommendations</b> .....	<b>46</b>
5.1. Powering the monolithic joint .....	46
5.2. Monolithic joint control .....	46
5.3. Recommendations .....	48
<b>Conclusion</b> .....	<b>50</b>
<b>List of references</b> .....	<b>51</b>
<b>Appendices</b> .....	<b>53</b>
Appendix 1. Alteration of inflatable bladder thickness (group X111) results .....	53
Appendix 2. Alteration of pseudo-rigid block area affected by pressure (group 1X11) .....	57
results .....	57
Appendix 3. Alteration of compliant element thickness (group 11X1) results .....	61
Appendix 4. Alteration of inflatable bladder material excess (group 111X) results .....	65

## List of figures

<b>Fig. 1.</b> Examples of 2D and 3D MEMS [1].....	12
<b>Fig. 2.</b> Examples of macro scale compliant mechanisms.....	12
<b>Fig. 3.</b> Compliant and pivot based motion comparison [2].....	13
<b>Fig. 4 .</b> Compliant bean with a Small –Length Flexural Pivot (SLFP) [2] .....	13
<b>Fig. 5.</b> A compliant segment and its chain elements [2] .....	14
<b>Fig. 6.</b> Examples of underactuated mechanisms .....	15
<b>Fig. 7.</b> Common types of Elastic Inflatable Actuators. [5] .....	15
<b>Fig. 8.</b> Common ways of introducing stiffness asymmetry [5].....	16
<b>Fig. 9.</b> Soft robotic griper before and after grasping an object [6].....	16
<b>Fig. 10.</b> Inflatable compliant joint design element.....	19
<b>Fig. 11.</b> Basic compliant joint design .....	21
<b>Fig. 12.</b> Design 1 (eccentric thickness design).....	21
<b>Fig. 13.</b> Design 2 (corrugated design) .....	22
<b>Fig. 14.</b> Design 3 (bellow design) .....	23
<b>Fig. 15.</b> Design 1 TangoBlack results .....	24
<b>Fig. 16.</b> TPU design 1 results .....	25
<b>Fig. 17.</b> Force produced by TPU design 1.....	26
<b>Fig. 18.</b> Deformation of TPU design 1 in z axis before and after external load is applied.....	26
<b>Fig. 19.</b> TPU design 2 results .....	27
<b>Fig. 20.</b> TPU design 2 additional results .....	28
<b>Fig. 21.</b> TPU design 3 results .....	29
<b>Fig. 22.</b> TPU design 3 additional results .....	30
<b>Fig. 23.</b> Design variant designation.....	32
<b>Fig. 24.</b> Variant 1111 results .....	33
<b>Fig. 25.</b> Variant 1111 results cont. ....	34
<b>Fig. 26.</b> The adjusted bladder thickness as compared to variant 1111 .....	35
<b>Fig. 27.</b> Bladder thickness effect on joint characteristics along with threndlines and their functions .....	36
<b>Fig. 28.</b> The adjusted pseudo-rigid block area affected by pressure as compared to variant 1111...	37
<b>Fig. 29.</b> Pressurized pseudo-rigid block area effect on joint characteristics along with threndlines and their functions.....	38
<b>Fig. 30.</b> The adjusted compliant element thickness as compared to variant 1111 .....	39
<b>Fig. 31.</b> Compliant element thickness effect on joint characteristics along with threndlines and their functions .....	39
<b>Fig. 32.</b> The adjusted bladder profile length as compared to variant 1111 .....	40
<b>Fig. 33.</b> Bladder profile length effect on joint characteristics along with threndlines and their functions .....	41
<b>Fig. 34.</b> Optimized variant 5555 as compared to variant 1111 .....	43
<b>Fig. 35.</b> Specialized combinations.....	44
<b>Fig. 36.</b> Combination 5155 with minor design revisions .....	45
<b>Fig. 37.</b> A Hall sensor size comparison [18] .....	47
<b>Fig. 38.</b> Monolithic, actuated joint with Hall sensor and a neodinium magnet snap fitted into place .....	47
<b>Fig. 39.</b> Strain propagation through the pseudo-rigid blocks .....	47



<b>Fig. 40.</b> Permanent magnet motion in relation to sensor .....	48
<b>Fig. 41.</b> Autonomous thermoactuator used to control greenhouse ventilation [19] .....	48
<b>Fig. 42.</b> Monolithic, actuated joints customized for specific applications .....	49
<b>Fig. 43.</b> Differential, monolithic, actuated joints .....	49
<b>Fig. 44.</b> Stabilizing platform using two electric motors [20] .....	49

## List of tables

<b>Table 1.</b> Primary testing conditions .....	18
<b>Table 2.</b> FEA testing setup conditions .....	20
<b>Table 3.</b> TangoBlack material properties.....	24
<b>Table 4.</b> TPU material properties.....	25
<b>Table 5.</b> TPU designs result summary .....	31
<b>Table 6.</b> Dimensional values of variant 1111 .....	33
<b>Table 7.</b> Results of variant 1111 .....	34
<b>Table 8.</b> Results of group X111 .....	35
<b>Table 9.</b> Results of group X111 compared in relation to baseline.....	36
<b>Table 10.</b> Results of group 1X11 compared in relation to baseline.....	37
<b>Table 11.</b> Results of group 11X1 compared in relation to baseline.....	39
<b>Table 12.</b> Results of group 111X compared in relation to baseline.....	40
<b>Table 13.</b> Summary of geometry-performance relations found during testing.....	42
<b>Table 14.</b> Benefit summary across all tested variants.....	43
<b>Table 15.</b> Results of combination variant 5555 .....	44
<b>Table 16.</b> Benefit comparison between baseline, highest individual and combination variants .....	44
<b>Table 17.</b> Results of revised combination variant 5155.....	45
<b>Table 18.</b> Benefit comparison between baseline, highest individual, combination 5555 and revised 5155 variants .....	45
<b>Table 19.</b> Variant 2111 results .....	53
<b>Table 20.</b> Variant 3111 results .....	54
<b>Table 21.</b> Variant 4111 results .....	55
<b>Table 22.</b> Variant 5111 results .....	56
<b>Table 23.</b> Variant 1211 results .....	57
<b>Table 24.</b> Variant 1311 results .....	58
<b>Table 25.</b> Variant 1411 results .....	59
<b>Table 26.</b> Variant 1511 results .....	60
<b>Table 27.</b> Variant 1121 results .....	61
<b>Table 28.</b> Variant 1131 results .....	62
<b>Table 29.</b> Variant 1141 results .....	63
<b>Table 30.</b> Variant 1151 results .....	64
<b>Table 31.</b> Variant 1112 results .....	65
<b>Table 32.</b> Variant 1113 results .....	66
<b>Table 33.</b> Variant 1114 results .....	67
<b>Table 34.</b> Variant 1115 results .....	68

## Introduction

Additive manufacturing allows not only for fast prototyping of conventional parts, but also for production of geometries previously considered impossible to manufacture. When considering what constructs could be made only by using this technology it becomes clear that compliant mechanisms would be the ideal design direction. Additive manufacturing and compliant mechanisms tend to compensate each other's weaknesses while making use of each other's strong points. This will be explained in more detail in the state-of-the-art overview. Thus, an exciting possibility, of producing an entire mechanism with a single manufacturing operation, presents itself. As it is not possible to preemptively say what mechanisms would be most viable for this design methodology, a more fundamental approach will be taken. An actuated joint is an inevitable part of any moving construct and it will be the focus of this study. And as this joint will not be assembled it will rely on geometry and material, both of which will be thoroughly investigated. This study should advance the understanding of monolithic mechanisms, serve as a reference for inflatable actuation design and motivate further investigations of additive manufacturing specific design.

Hypothesis: Could functional, powered, monolithic mechanisms be designed, allowing for manufacturing by a single operation (additive manufacturing).

Aim: Investigate the viability of a monolithic, actuated joint and compile a set of design notes describing the influence of geometry and material over the performance of said joint.

Project tasks:

1. Model a set of overall design variations and test the variations using finite element analysis, determining the most promising design.
2. Refine the most optimal design variation keeping note of geometry-performance correlations.
3. Propose methods of control, propulsion and possible application for the developed joint.

## 1. State-of-the-art overview

### 1.1. Compliant mechanisms

Compliant designs are mostly used to reduce construction complexity and weight. Compliant mechanisms are currently used in MEMS (Fig. 1.) due to their miniaturization possibilities.

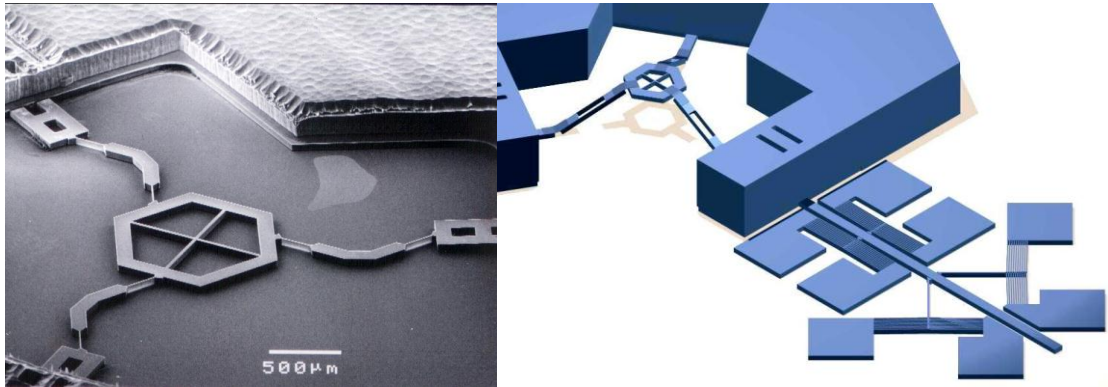
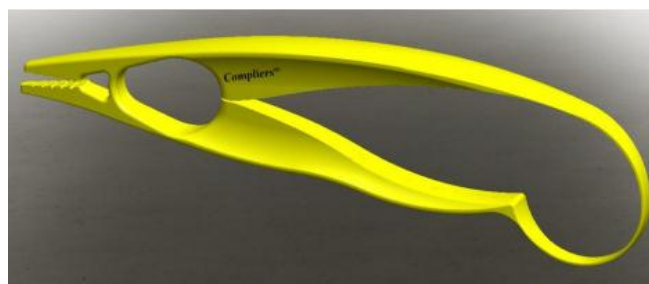
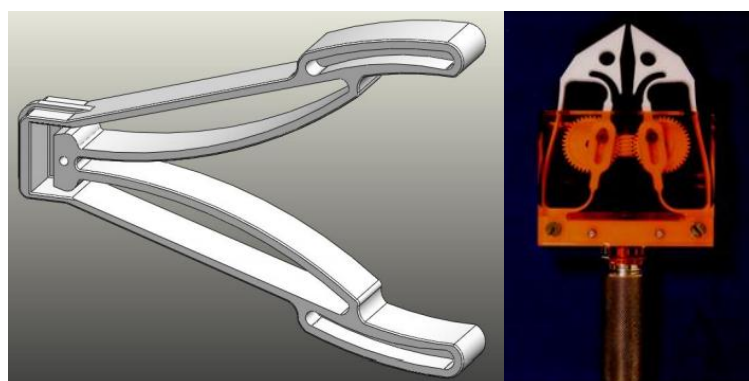


**Fig. 1.** Examples of 2D and 3D MEMS [1]

While compliant mechanisms are the only approach available when developing micro mechanical constructs (Fig. 2), they can also be used for macro structures.



a)



b)

c)

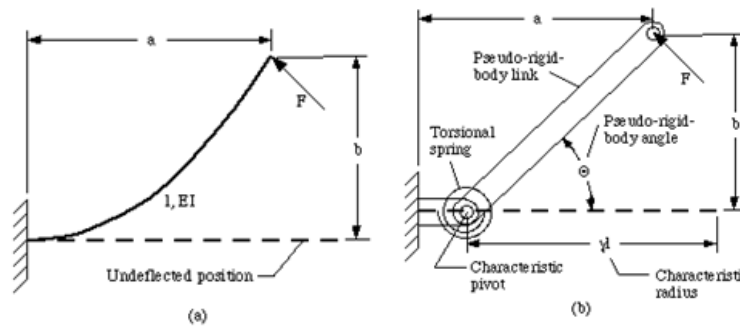
**Fig. 2.** Examples of macro scale compliant mechanisms: a) Compliers®; b) crimping mechanism; c) compliant gripper [2]

### 1.1.1. Implications of compliant mechanisms

From a mechanical standpoint, compliant mechanisms offer multiple advantages specific to this method of energy transfer:

- Lack of bearing surfaces removes the necessity of mechanism lubrication and reduces overall surface smoothness requirements.
- Without multiple parts that would introduce errors through fit tolerances the overall precision of the mechanism is increased.
- Due to direct influence geometry has over motion, complex trajectories can be achieved even with minimalistic designs.

This approach is considerably more complicated in terms of kinematics because the actual axis of joint rotation is not as clear. While a typical hinge can be considered as a point of zero stiffness connecting two or more rigid elements a compliant joint deforms to allow motion (Fig. 3). This difference changes the kinematic motion of the system as the point of rotation is replaced by angular motion being distributed along the low stiffness area.



(a) A flexible segment and (b) its pseudo-rigid-body model.

**Fig. 3.** Compliant and pivot based motion comparison [2]

This leads to motion non-linearity as points of flexible area reach higher strain, their stiffness increases and the point of bending moves to a less strained portion of the flexible area. In addition, end point trajectory during rotation is no longer limited to a beam length defined radius. This problem is often addressed by reducing the length of flexible area to a small-length flexural pivot (SLFP) and treating the rest of the beam as a rigid element (Fig. 4).

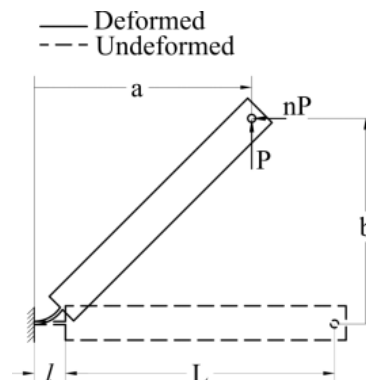


**Fig. 4 .** Compliant beam with a Small –Length Flexural Pivot (SLFP) [2]

Such limitation makes compliant mechanism more similar to pivot type joint with axis of rotation being vaguely defined.

Compliant joints do have a key benefit when considering their actuation and control. A traditional pivot does not resist torque applied to it and in theory would continue to rotate indefinitely if a force is applied to it. A compliant joint is akin to traditional pivot with an incorporated spring. This means that unlike a rotational pivot, compliant joint:

- Can maintain its angle if external forces are minimal (acts as a joint break if surrounding element masses are low compared to joint stiffness).
- Naturally resists forces applied to it. This allows the control of joint angle with single input of force and no additional elements. The resistance force provided by the joint stiffness reaches an equilibrium with the external force at a certain angle and this angle can change by adjusting only the external force.

It should be noted that compliant elements, much like conventional ones, have provided a wide range of fatigue resistance results, from a few hundred cycles to one million and more [3]. As such compliant elements should not be considered inferior in terms of service life by default.

### 1.1.2. Calculation of compliant mechanisms

Regardless of the construction approach chosen the motion of the flexible area can only be calculated by considering it as a chain of rigid-body elements with rotation evaluated for each node connecting these elements (Fig. 5).

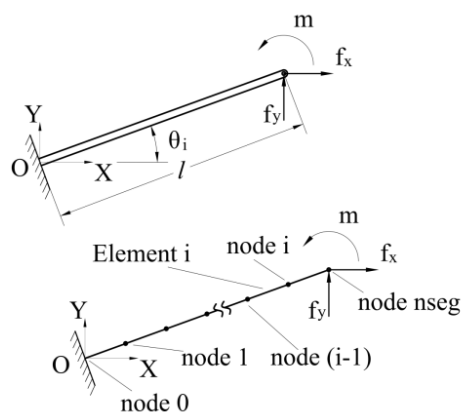


**Fig. 5.** A compliant segment and its chain elements [2]

This is basically a method of finite element analysis (FEA) with each node being defined as a set of displacement formulas and the accuracy of these calculations being directly tied to the number of elements. Because of this, a mathematical model of such joint is very cumbersome and can only realistically be performed by virtual simulations.

### 1.1.3. Underactuation of compliant mechanisms

Compliant mechanisms are generally underactuated. Underactuated mechanisms are mechanisms with fewer actuators than degrees of freedom. Through more complex transmission systems, these constructs can provide motion to multiple joint utilizing a single point of energy input (Fig. 6.). Compliant mechanisms often rely on underactuated constructions due to lack of shafts that could be

connected to sources of torque. This makes compliant mechanisms even more minimalistic in terms of used parts and helps maintain constructs accuracy even with multiple degrees of freedom.

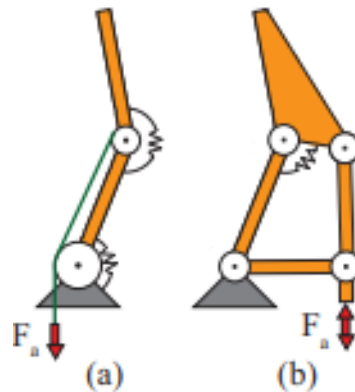


**Fig. 6.** Examples of underactuated mechanisms: a) cable-driven system; b) linkage driven system [4]

## 1.2. Inflatable actuators

There is a rather wide range of application for compliant mechanisms with multiple joints, but the transmissions necessary to power them mechanically can be cumbersome. A fluid based method of actuation could remove the need for transmission by providing energy to the mechanisms either by individual joints or even by single port. The most prominent example of pneumatic compliant mechanisms can be seen in soft robotics.

Soft robot designs rely on flexible hollow profiles being pressurized [5]. Most examples of these elastic inflatable actuators (EIA) (Fig. 7.) provide axial force. A bellow type design is most simplistic and allows actuator to expand when pressurize. A pneumatic artificial muscle (PAM) is a contracting axial actuator than transforms its radial expansion to axial contraction through the use of strain limiting fibers. These fibers are often incorporated in soft robotics designs as they provide constrains allowing to direct the deformation of inflatable elements. With these fibers torsion and bending motions can also be achieved with EIAs.

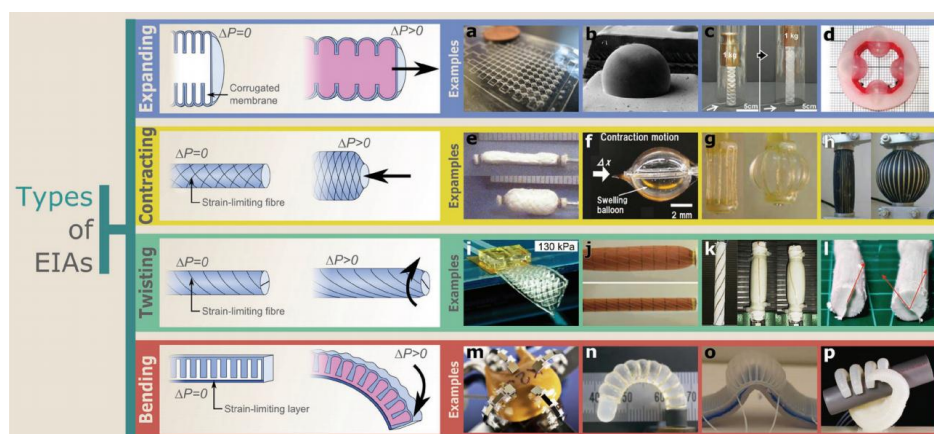


**Fig. 7.** Common types of Elastic Inflatable Actuators. [5]

Bending actuation is rarely used in conventional mechanisms but are at the core of most soft robots. While most popular, axial actuation is often combined with torque levers to rotate a joint and a torque actuator can more directly be used to the same effect. However, compliant mechanisms already

replace rotation with bending, therefore, using a bending actuation type can simplify the mechanism design by removing transmissions that would be necessary otherwise.

Bending actuation is almost universally achieved through asymmetrical profile stiffness (Fig. 8). This can be done by increasing the stiffness of a specific area either by increasing material thickness or the composition of material itself. Analogically the opposite approach of reducing stiffness of an area can also be taken by increasing the surface area.

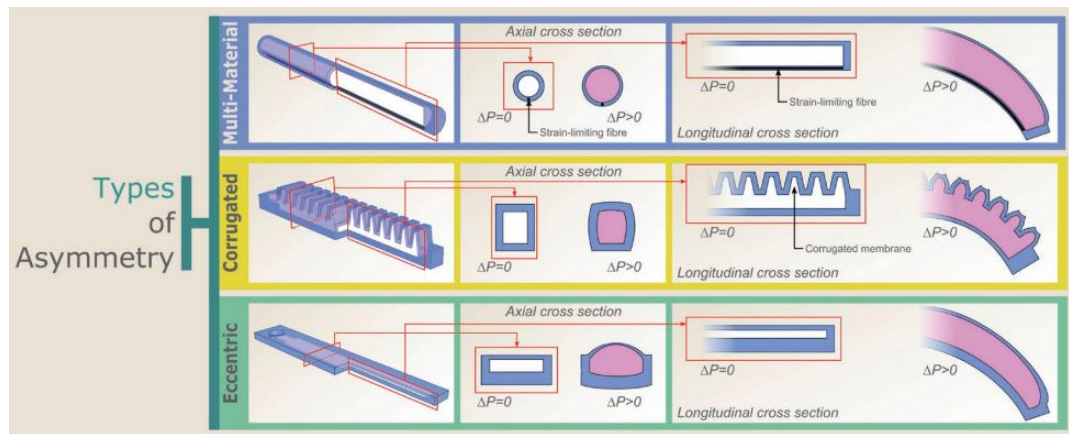


**Fig. 8.** Common ways of introducing stiffness asymmetry [5]

While multi-material method is the most compact it removes the benefit of a monolithic construct. Soft robots are mostly known for their safe interaction with humans and same non-rigid properties tend to be beneficial when handling fragile, easily deformable objects. However, the common “tentacle” design for soft robotic griper fingers is not very reliable in terms of accuracy. As soft grippers adjust to the shape of the object and have many degrees of freedom it is not uncommon for more universal soft grippers to rotate the part in question during clamping (Fig. 9.). This in turn makes them incapable of reliably orientating parts for production or assembly.

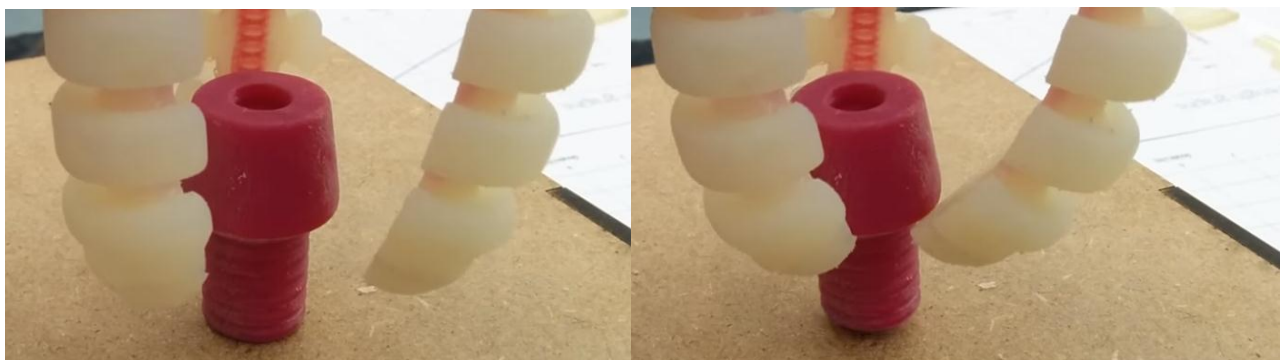


**Fig. 9.** Soft robotic griper before and after grasping an object [6]

### 1.3. Additively manufactured compliant actuators

Compliant pneumatically controlled mechanisms offer unique benefits and may be applied to a wide variety of industries but designing them is a complicated process especially when considering manufacturing challenges presented by these lean and covetous constructs.

In recent years, production of unique and complex geometries has been steadily taken over by additive manufacturing (AM). AM introduced the possibility to produce geometries that were considered



either technologically impossible or economically not viable. 3D printing is particularly beneficial to soft robotics and compliant mechanisms in general and will undoubtedly accelerate the development of both fields. While compliant mechanisms 3D printed from nylon have been relatively well discussed by the scientific community, with new printable material being constantly introduced possibility of additively manufactured, flexible robotics becomes more realistic. Materials such as FormLabs Flexible (~80% elongation) [7], Tango Black (~200% elongation) [8] and Silicon rubber (400% elongation) are a few of rubber-like materials available for 3D printing. With this state-of-the-art additively manufactured, inflatable elements are producible.

Pneumatically actuated, compliant mechanisms have been developed in the past [9]. While not entirely monolithic the gripper developed in the article was actuated entirely by inflation of pseudo flexible, 3D printed, PA2200 (nylon 12) polyamide coils. Axels were necessary to achieve desired motion, but without the limitation of plastic as material of choice it could be possible to develop entirely compliant, monolithic gripper.

#### **1.4. State-of-the-art overview summary**

Compliant mechanisms are considerably underdeveloped part of engineering when compared to conventional mechanisms. This is mostly the consequence of complicated manufacturing processes necessary to produce complex compliant constructs. With the current advances in the field of additive manufacturing industrial production of compliant mechanisms has become considerably more viable. The benefits introduced by compliant, monolithic actuators make this a promising field of study, especially with additive manufacturing relieving manufacturing problems.

Most prominent use of macro scale compliant mechanisms in the industry can be seen in the field of soft robotics. Soft grippers and actuators are generally not only utilizing basis of compliant design, but also improve on the concept with the use of flexible materials. Soft actuators are generally powered pneumatically creating the concept of elastic inflatable actuators. Compliant joints powered pneumatically, with asymmetric stiffness in mind are at the core of soft gripper design. However due to high degree of freedom these grippers are not accurate.

Material such as Nylon 12 and Ti6Al4V will likely remain the primary materials of choice for additive manufacturing. However, more variations of flexible materials for 3D printing have been introduced in the recent past. With these materials monolithic 3D printed parts can be better used for motion transfer and actuation. The engineering field of soft robotics has greatly benefited from these advances, developing complex, flexible grippers and actuators with little concern for difficult geometry.

More research should be done in terms of constrained soft robotics. Using complex geometry to introduce variable rigidity to a monolithic construct therefore fully utilizing the benefits of additive manufacturing. In this manner, more conventionally functioning mechanisms might be developed with the benefits of compliant joints and EIAs in single part mechanisms made possible by 3D printing of flexible materials.

## 2. Design testing

### 2.1. Method and equipment

The purpose of the following finite element analysis is to evaluate possible designs for monolithic, compliant, inflation actuated joint. This is a comparative study, therefore, no specific application for the designs will be considered during development. The designs will not be loaded with equivalent loads, but rather loaded to the point of structural failure to determine their capabilities.

Some aspects of the design remain constant, such as the overall size of the joint, thickness of the compliant area of the joint and external load applied to the joint.

Variable aspects for testing are materials used, actuating geometry and pressure used for inflation. Flexible materials of varying stiffness were considered for the designs: Thermoplastic Polyurethane (TPU) (elongation ~55% [10]); TangoBlack (elongation ~218% [11]); Silicone rubber (elongation ~400%). As different materials have different tensile yield the pressure for inflation is chosen individually to demonstrate the potential of each design.

Designs have been evaluated in terms of numerical parameters. Change of angle after joint inflation illustrated the range of motion provided by the design. Force produced by pressure equivalent to that necessary to achieve maximum angle. Considering that different joints provide different range of motion, the maximum force produced at starting angle (30°) has been compared. Finally, an external load has been applied in a direction where joint freedom is considered constrained. This is done to determine the overall rigidity of the system. These conditions can be found in Table 1.

**Table 1.** Primary testing conditions

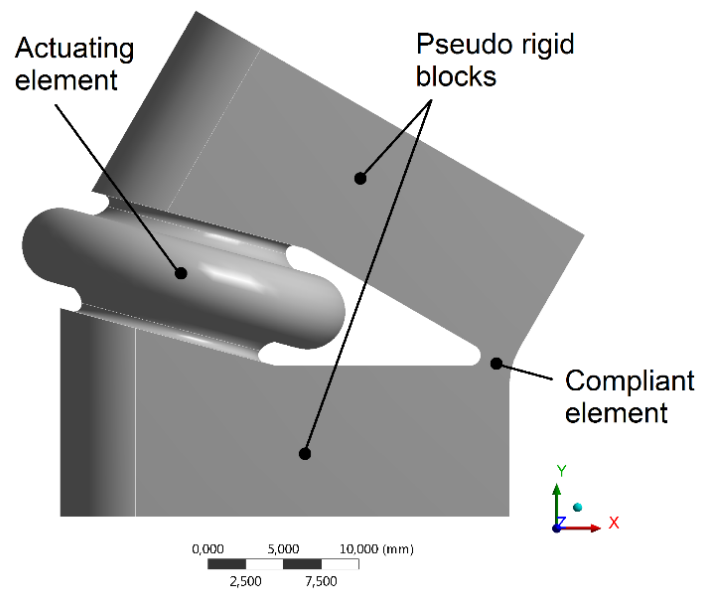
Constants	Variables	Parameters of interest
Overall size	Material used	Displacement created by actuation (°)
Minimum thickness of compliant area	Geometry of the inflatable element	Force created by actuation (N)
External load	Pressure used for inflation	Deflection created by external load (mm)
Monolithic nature of the design		

SOLIDWORKS 2017 was the parametric modeling program used to create the joint designs. ANSYS Workbench 18.1 was the FEA program used for the comparative tests.

The testing process:

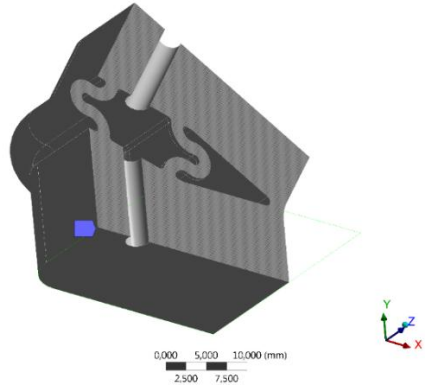
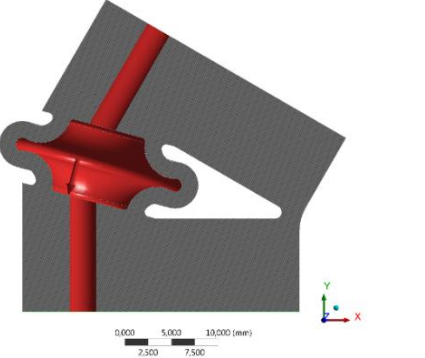
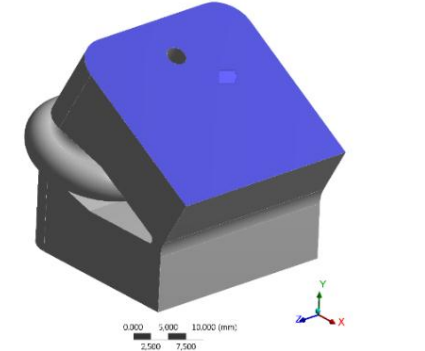
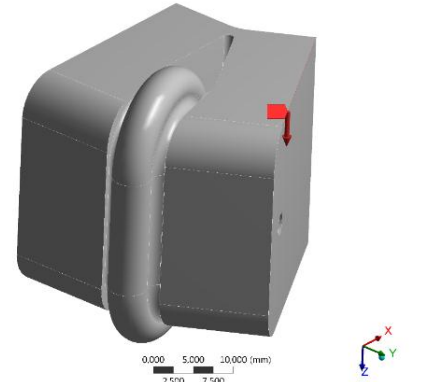
1. Eccentric thickness design (design 1) has been tested using TangoBlack material to determine viability of the material.
2. TangoBlack is an intermediate material between TPU and Silicon rubber in terms of flexibility. Depending on its overall performance a more rigid or less rigid material has been chosen for further testing. The other material was considered unfit without testing.
3. When a viable material was determined all 3 fundamentally different designs were tested.

For future reference designation of fundamental design elements is provided in Fig. 10. All tests had been setup following the conditions described in Table 2.



**Fig. 10.** Inflatable compliant joint design element

**Table 2.** FEA testing setup conditions

Description	Illustration
<p>The perimeter of one side of the pseudo rigid joint blocks has been fully constrained. This maintains a stable base for reference while allowing for expansion of the air supply channel.</p>	
<p>Pressure is applied to all internal surfaces of the design. Stress, deformation and achieved angular motion are recorded.</p>	
<p>Calculations are repeated with the previously unconstrained surface being fully constrained to determine the reaction force produced by actuation. After the force has been recorded this constrain is removed.</p>	
<p>In addition, a force whose direction matches that of the joints axis of rotation is applied. The resulting deformation determines how susceptible joint is to loads not related to actuation.</p>	

## 2.2. Geometrical basis design

A simple compliant joint was used as a basis for all designs (Fig. 11.). The size of the joint and the minimum 2mm thickness of the compliant area (A) remains constant in all designs.

The joint has a starting angle of  $30^\circ$  in order to ensure that the compliant area (A) is minimal while providing a space for actuating design between the two relatively moving pseudo rigid blocks. Compliant area is minimized in hopes of reducing the degrees of freedom provided by the compliant element allowing it only to rotate.

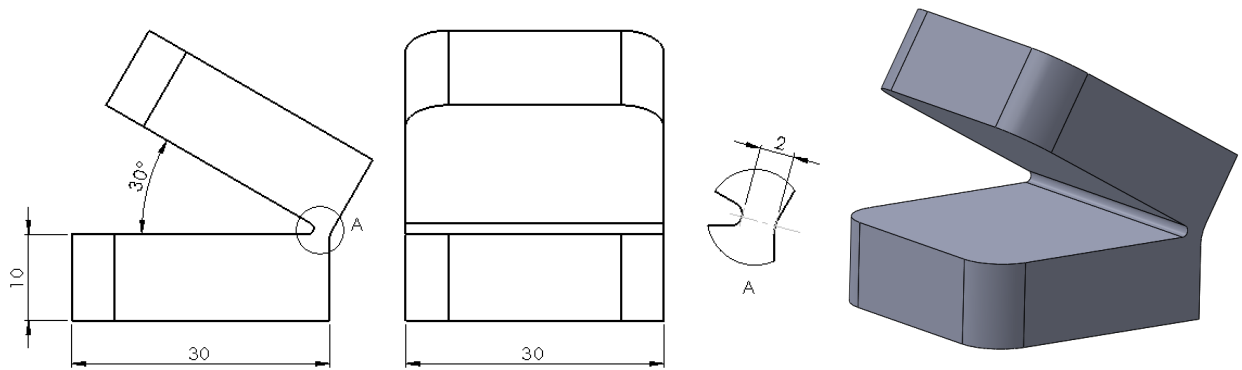


**Fig. 11.** Basic compliant joint design

Using the basis design, three design variations for actuation have been modeled. Variations were based on geometries applied in soft robotics. These variations will be referred to as design 1, 2 and 3.

### 2.2.1. Eccentric thickness design (design 1)

The first design (Fig 12.) is based on the concept of eccentric thickness used in bending actuation for soft robotics. The implications of this design are that pressure will increase the joint angle by stretching the thin material surrounding the previously shown fundamental design.

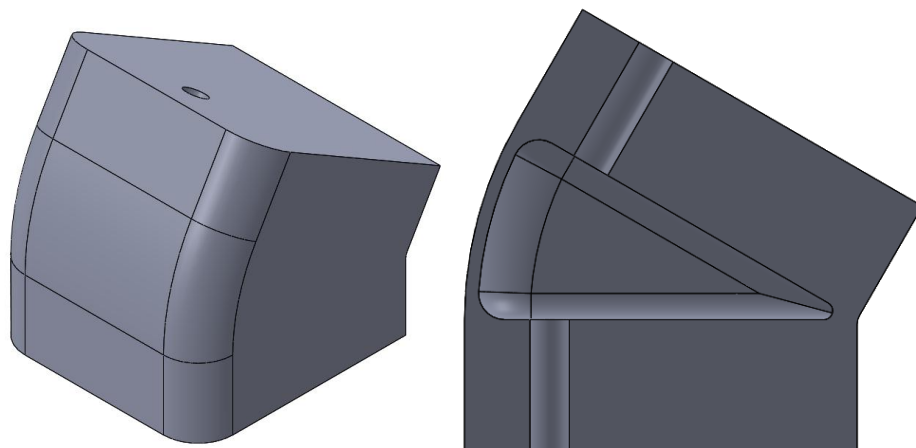


**Fig. 12.** Design 1 (eccentric thickness design)

Initial design pros and cons:

+ Geometrically simple;

- + Compliant and actuating elements are combined;
- Design heavily relies on material elongation rather than bending flexibility;
- Material will experience higher strain the further it is from the compliant element;
- Unlikely to provide large angular motion.

### 2.2.2. Corrugated design (design 2)

This design, same as the first is borrowed from bending soft robotic actuators and achieves rotation through geometrical asymmetry. However, this model uses a corrugated wall design to provide an excess of material and ease deformation. (Fig. 13.)

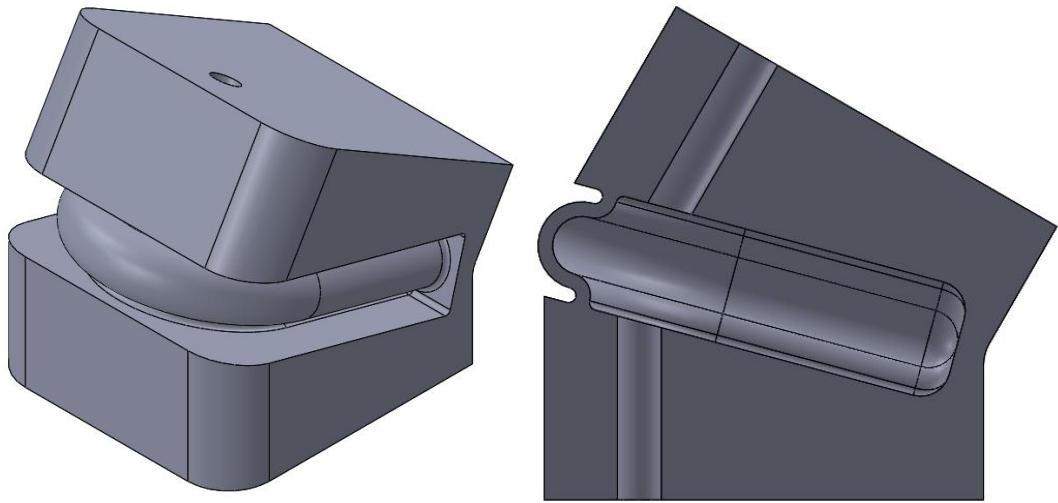


**Fig. 13.** Design 2 (corrugated design)

Initial design pros and cons:

- + Compliant and actuating elements are combined;
- + Design relies on material bending flexibility rather than elongation;
- More complex geometry;
- Material will experience higher strain the further it is from the compliant element;
- Poorly defined compliant area.

### 2.2.3. Bellow design (design 3)

Last design is no longer based around bending inflatable actuators, but instead uses a bellow design common in expanding linear motion inflatable actuators. This completely separates compliant and actuating elements of the joint. It uses an expanding bellow to actuate the joint and the compliant area to translate this expansion into rotation. (Fig. 14.)

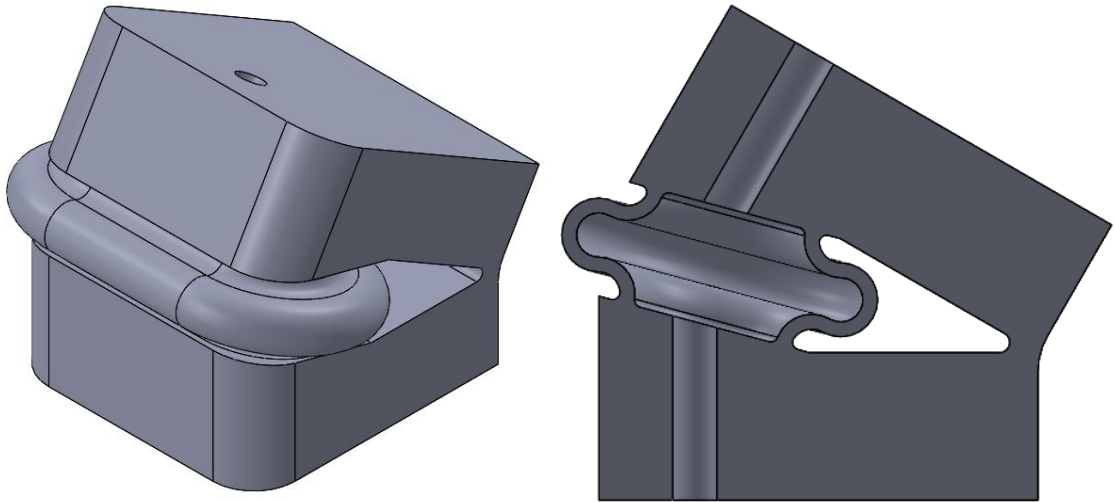


**Fig. 14.** Design 3 (bellow design)

Initial design pros and cons:

- + Material will experience similar strain throughout the actuating element.
- + Design relies on material bending flexibility rather than elongation;
- Compliant and actuating elements are separate;
- Complex geometry;
- Consumes the largest amount of material.

### 3. Results

#### 3.1. Design 1 TangoBlack

For the following test TangoBlack (Tango Black Full-Cure 930) 3D printable material (Table 3.) was used:

**Table 3.** TangoBlack material properties

TangoBlack Full-Cure 930 material properties [11, 12, 13]	
Young's modulus (MPa)	0.722
Poisson's ratio	0.49
Tensile strength (MPa)	1.455

The first design was inflated with a pressure of 0.035 MPa resulting in stress of 1.41MPa (Fig 15. a) and total deformation of 24.04 mm (Fig 15. b)). Whether this is the way material would inflate or a mathematical error is unclear, however under these conditions angle of achieved rotation cannot be determined.

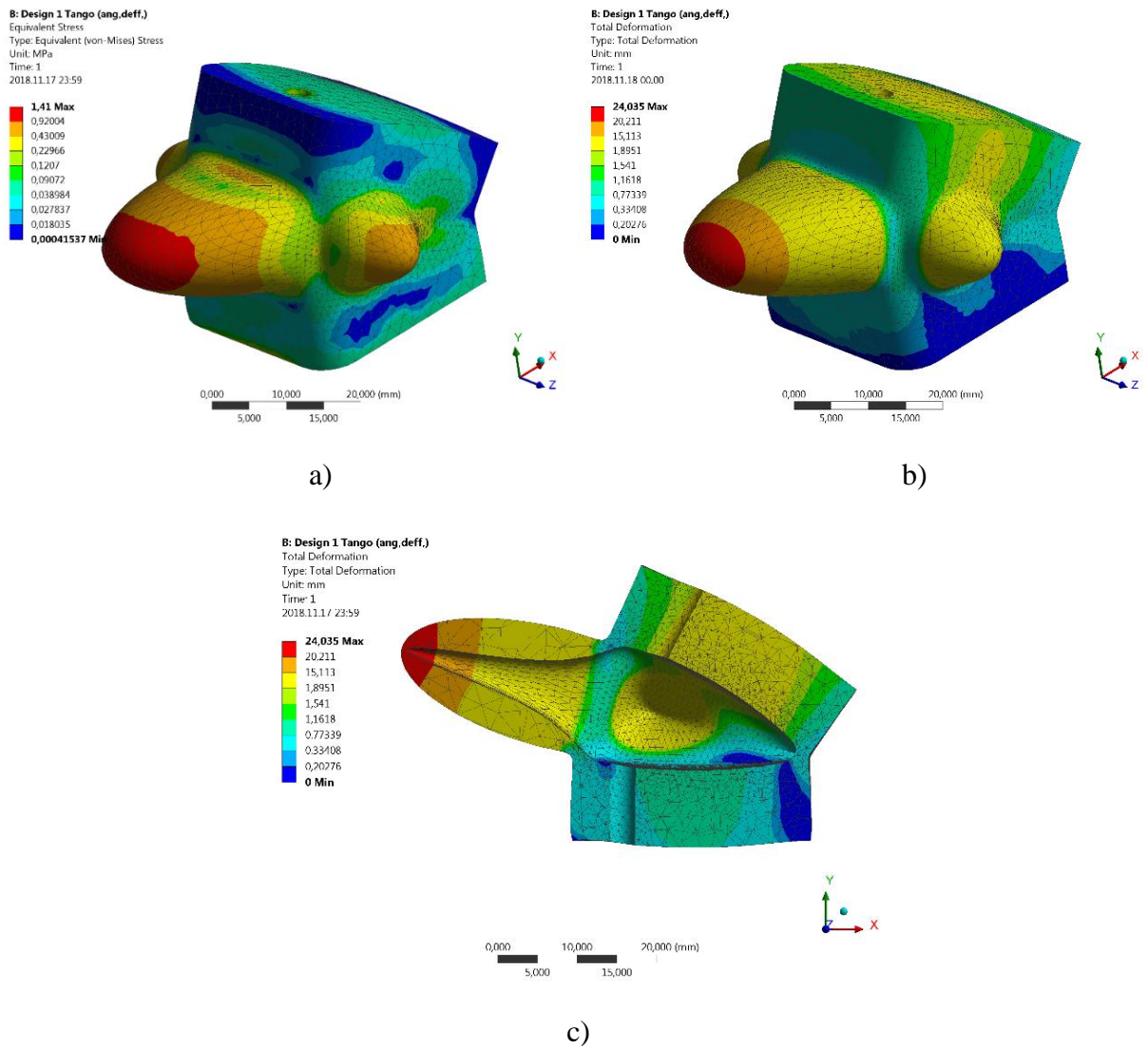


**Fig. 15.** Design 1 TangoBlack results: a) stress results; b) deformation results; c) deformation results cross section



Due to such extensive deformations at low pressure it has been concluded that TangoBlack is not a suitable material for this application due to extremely low rigidity. Study of designs made from Silicon rubber have also been canceled because the rigidity of latter material is theoretically even lower than that of TangoBlack.

### 3.2. Design 1 TPU

For the following tests Thermoplastic Polyurethane (TPU 95A) 3D printable material (Table 4.) was used:

**Table 4.** TPU material properties

TPU 95A material properties [10, 14]	
Young's modulus (MPa)	26
Poisson's ratio	0.49
Tensile yield stress (MPa)	8.6
Tensile ultimate stress (MPa)	39

The first design was inflated with a pressure of 0.2 MPa resulting in stress of 8.54 MPa (Fig 16. a)) and total deformation of 3.859 mm (Fig 16. b)). From deformation the achieved rotation angle can be determined (Fig. 16. c)). In the case of design 1, however no discernable angular motion has been achieved.

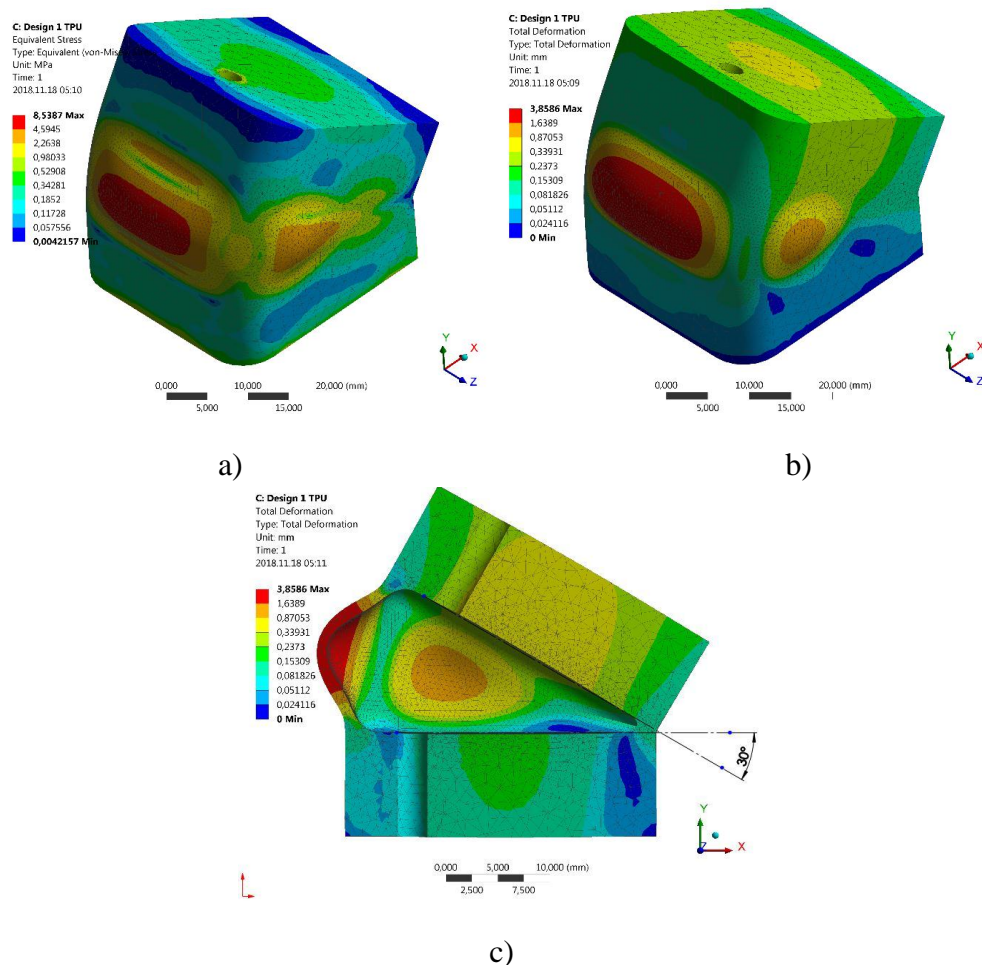


**Fig. 16.** TPU design 1 results: a) stress results; b) deformation results; c) deformation results cross section

Due to outer surfaces still being deformed by applied pressure, force of 46.13 N (Fig. 17.) has been generated. The external load test revealed a deformation difference (Fig. 18.), in the direction of applied force, at a point located in the unconstrained pseudo rigid block to be 0.288 mm under the load of 10 N. This force value was chosen to imitate approximately 1 kg load in the theoretical axis of rotation and is primarily used as a constant for comparison.

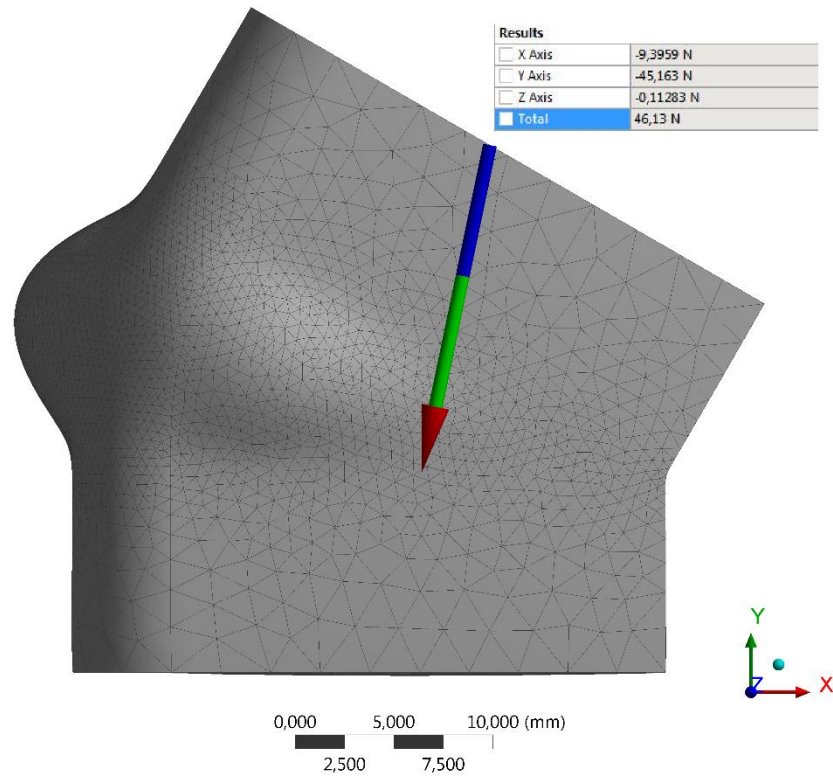


**Fig. 17.** Force produced by TPU design 1

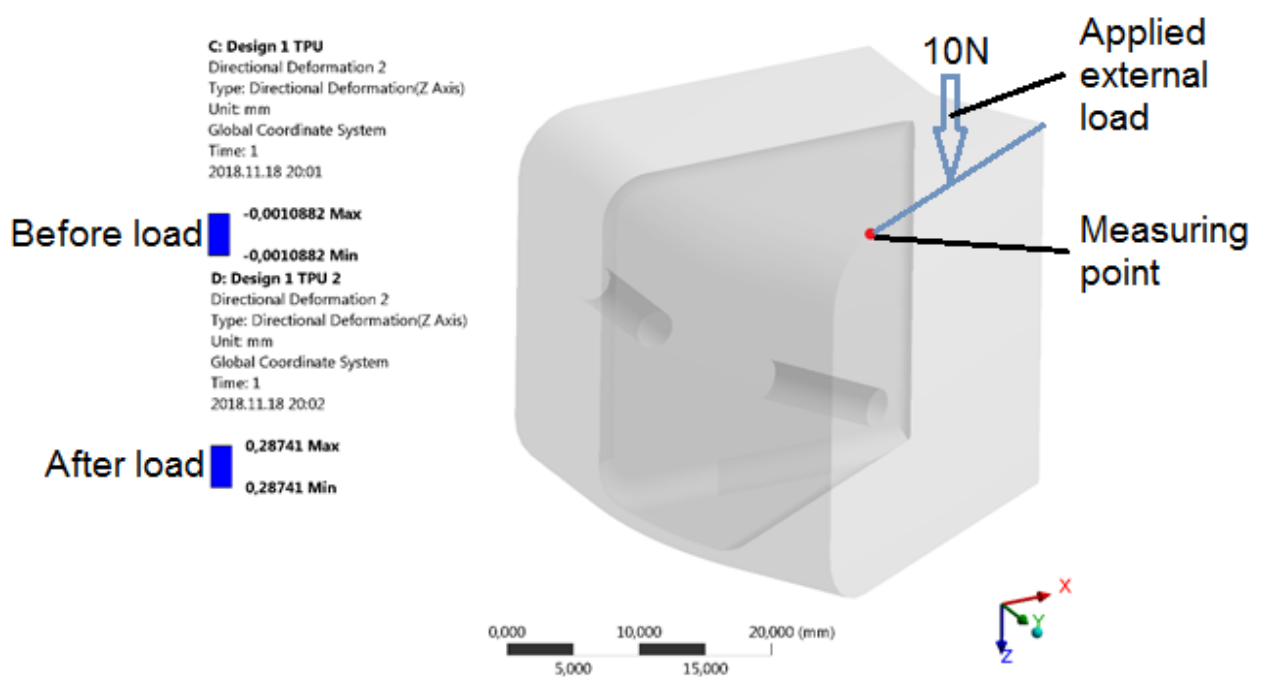


**Fig. 18.** Deformation of TPU design 1 in z axis before and after external load is applied

To summarize the results of design 1 it was determined that no practical functionality has been achieved due to lack of rotation. However, TPU material had proven rigid enough to withstand not only a reasonable amount of pressure (in terms of soft robotics [15]), but also a considerable external load without extensive deformation. Considering this partial success, the next design was tested.

### 3.3. Design 2 TPU

Design 2 was inflated with a pressure of 0.11 MPa resulting in stress of 8.56 MPa (Fig. 19. a)) and total deformation of 4.291 mm (Fig 19. b)). From deformation the achieved rotation angle of 7.54° has been determined (Fig 19. c), d)).

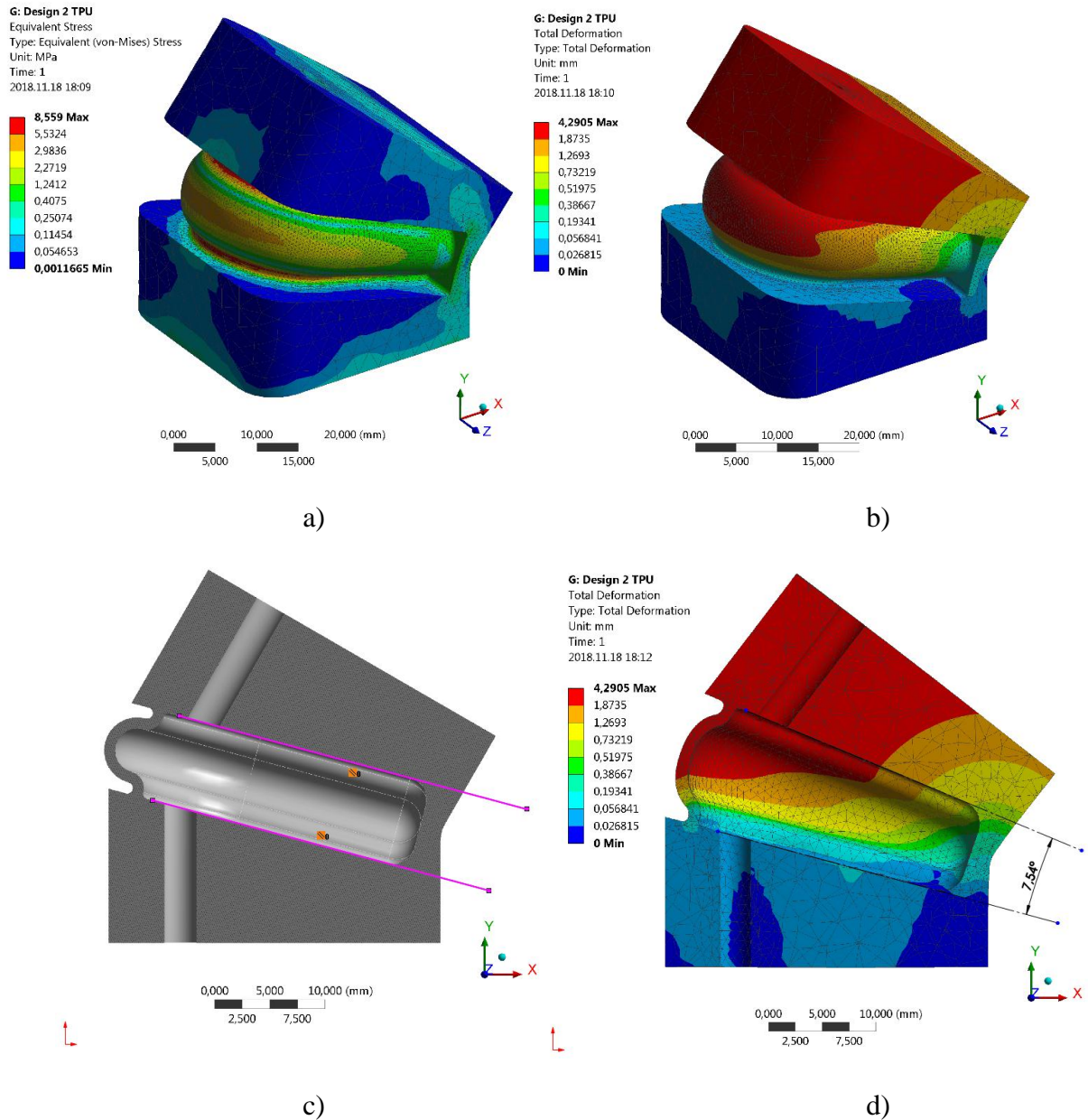
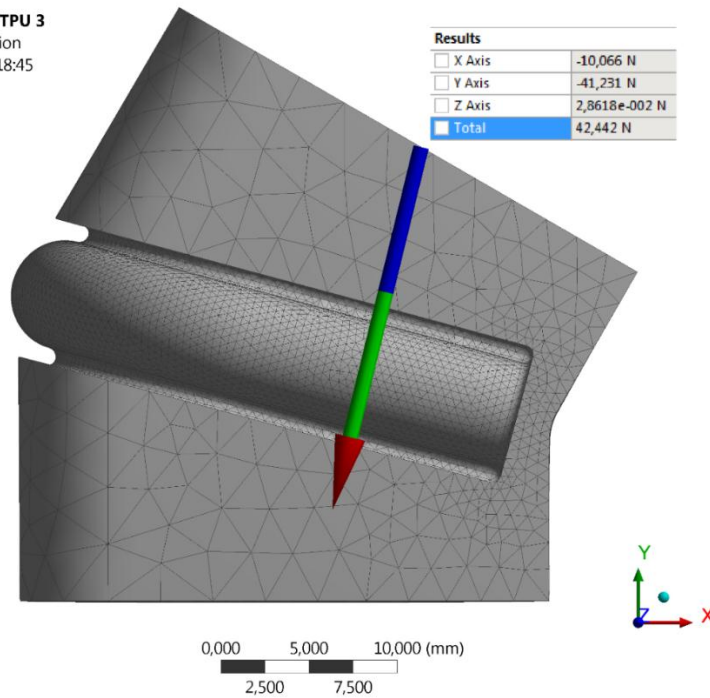


**Fig. 19.** TPU design 2 results: a) stress results; b) deformation results; c) cross section before deformation; d) deformation results cross section

The actuation produced by pressurized design 2 resulted in generated force of 42.442 N (Fig 20. a)). The external load test revealed a deformation difference, in the direction of applied force, to be 0.588 mm under the load of 10 N (Fig 20. b)).

I: Design 2 TPU 3  
Force Reaction  
2018.11.18 18:45



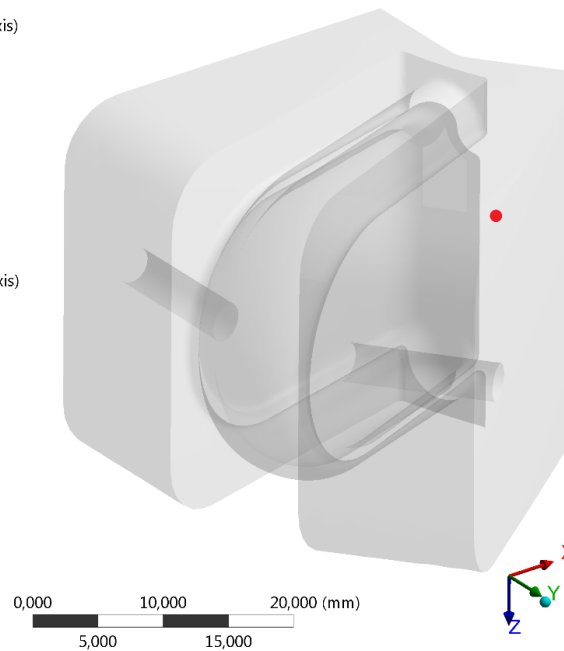
a)

G: Design 2 TPU  
Directional Deformation 2  
Type: Directional Deformation(Z Axis)  
Unit: mm  
Global Coordinate System  
Time: 1  
2018.11.18 20:09

0,015346 Max  
0,015346 Min

H: Design 2 TPU 2  
Directional Deformation 2  
Type: Directional Deformation(Z Axis)  
Unit: mm  
Global Coordinate System  
Time: 1  
2018.11.18 20:10

0,60347 Max  
0,60347 Min



b)

**Fig. 20.** TPU design 2 additional results: a) force produced; b) deformation in z axis before and after external load is applied

To summarize the results of design 2 it was determined that a corrugated actuating element design allows for rotation to be achieved rendering such design viable for practical application. The TPU material continues to provide acceptable rigidity. While the inflating pressure at rupture has been reduced to 55% of that used with design 1, the force produced by this actuator was 92% that of design 1.

### 3.4. Design 3 TPU

Design 3 was inflated with a pressure of 0.11 MPa resulting in stress of 8.59 MPa (Fig. 21. a)) and total deformation of 7.799 mm (Fig. 21. b)). From deformation the achieved rotation angle of 14.53° has been determined (Fig. 21. c), d)).

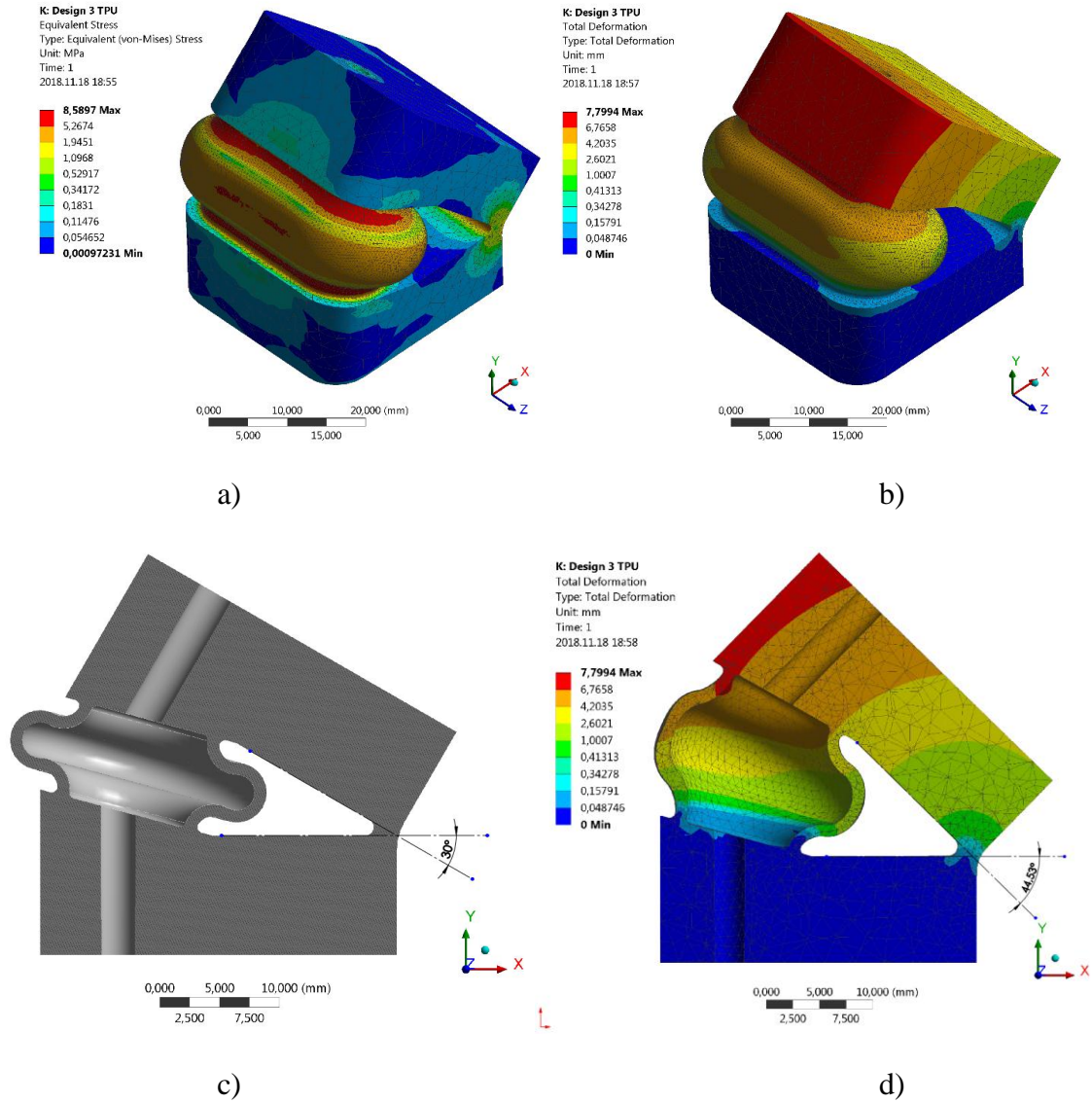
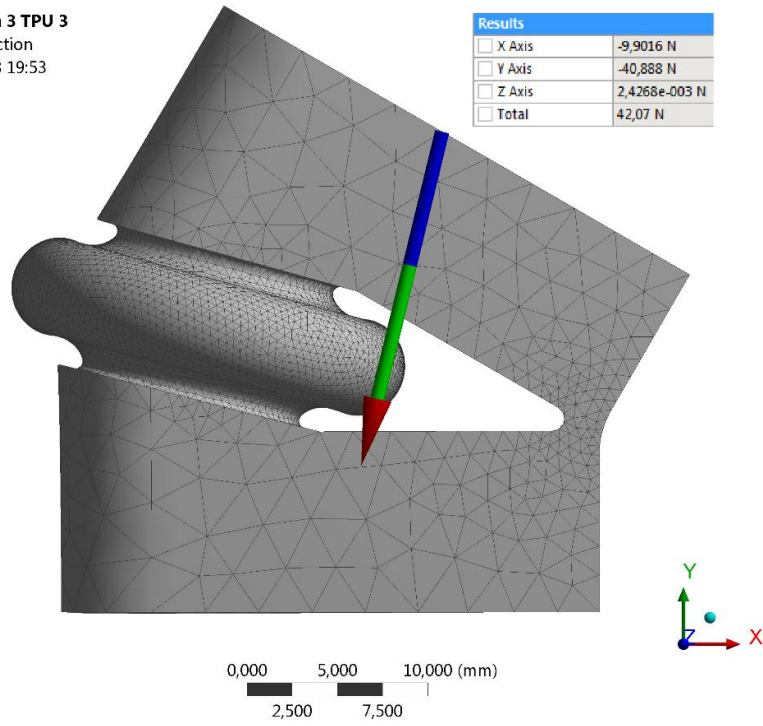


**Fig. 21.** TPU design 3 results: a) stress results; b) deformation results; c) cross section before deformation; d) deformation results cross section

The actuation produced by pressurized design 3 resulted in generated force of 42.07 N (Fig. 22. a)). The external load test revealed a deformation difference, in the direction of applied force, to be 0.472 mm under the load of 10 N (Fig. 22. b)).

M: Design 3 TPU 3  
 Force Reaction  
 2018.11.18 19:53

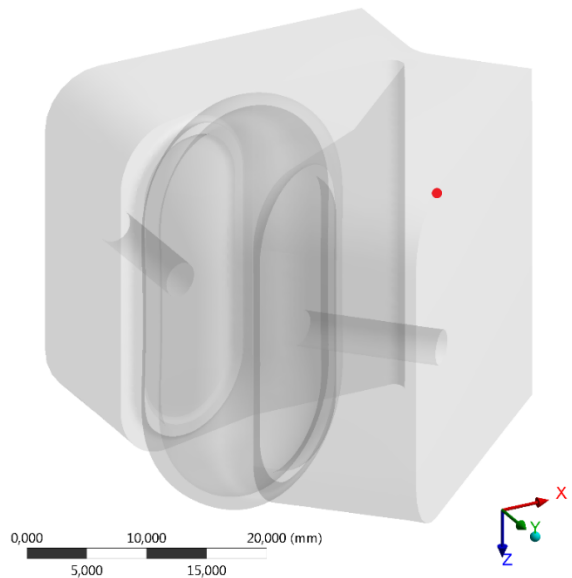


a)

K: Design 3 TPU  
 Directional Deformation 2  
 Type: Directional Deformation(Z Axis)  
 Unit: mm  
 Global Coordinate System  
 Time: 1  
 2018.11.18 20:14

-0,00831 Max  
 -0,00831 Min  
 L: Design 3 TPU 2  
 Directional Deformation 2  
 Type: Directional Deformation(Z Axis)  
 Unit: mm  
 Global Coordinate System  
 Time: 1  
 2018.11.18 20:14

0,46354 Max  
 0,46354 Min



b)

**Fig. 22.** TPU design 3 additional results: a) force produced; b) deformation in z axis before and after external load is applied

To summarize the results of design 3 it was determined that, similarly to the corrugated actuating element design, the independent bellows allows for rotation to be achieved rendering such design viable for practical application. Furthermore, the produced angle of rotation was 193% that of design 2 despite using the same 0.11 MPa pressure. In addition, while the produced actuating force remained similar to that of design 2, unwanted deflection of the joint when an external force is applied was reduced by 20%.

### 3.5. Overall design study results

The results provided in this study are not comparable to physical test results and the observed parameters should not be considered an accurate prediction of manufactured designs. FEA does not consider a variety of real-life factors such as geometric imperfections, material homogeneity and so on. These results do provide a frame of reference when comparing different geometrical designs under identical virtual conditions. The acquired results have been systemized in Table 5, only TPU results were used due to their viability.

**Table 5.** TPU designs result summary

	TPU 95A		
	Design 1	Design 2	Design 3
Pressure applied before structural failure (MPa)	0.2	0.11	0.11
Angle produced by inflation (°)	0	7.54	14.53
Force produced by actuation (N)	46.13	42.442	42.07
Deformation due to external 10 N load (mm)	0.288	0.588	0.472

While design 1 proved to be the most rigid its complete lack of motion proves it to be ineffective as an actuated joint.

Design 2 was considered viable due to produced angular motion. The corrugated design introduced excess material that while allowing for rotation reduced joint rigidity. The pressure used had to be significantly reduced when compared to design 1. This was likely caused by considerable increase in actuating element surface area provided by the thin walls, resulting in thinnest parts of the design receiving most of the pressure load.

Design 3 is considered the most optimal in comparison to others. Its bellow design is similar to the corrugated geometry of design 2, which is likely the cause for them sharing a pressure threshold. Design 3 is unique in having its compliant and actuating elements separated. This lack of conflict between expanding and rotating parts is likely the cause of significantly higher joint rotation angle. Due to the favorable orientation of the expanding chamber, design 3 was less susceptible to external load. Force produced by the joint remained similar between designs 2 and 3.

#### 4. Investigation of design geometry

With the most effective of the three designs determined, a more in-depth investigation can be performed. As only one of the considered materials has been proven viable, only the relations between joint characteristics and dimensions of joint key elements remain unclear. The following is a compilation of test investigating design geometry effect on actuation characteristics. These tests have been performed analogically to the ones described in chapters 2 and 3 in order to maintain data consistency.

##### 4.1. Testing process

The three joint characteristics in question are actuation angle, force and deflection same as in previous chapters. In this case design 3 (bellow design) has undergone minor systematic changes of geometry dimensions. The geometric elements that were altered are:

1. Thickness of the inflatable bladder;
2. Area of pseudo-rigid block affected by pressure;
3. Compliant element thickness;
4. Inflatable bladder excess material.

Significance of each of these elements will be explained in sections 4.3.-4.6. Each of the dimensions had a 5 variant sample size in order to establish trends from calculated results. Because of the large total number of variations, a four-digit designation system has been used (Fig. 23.).

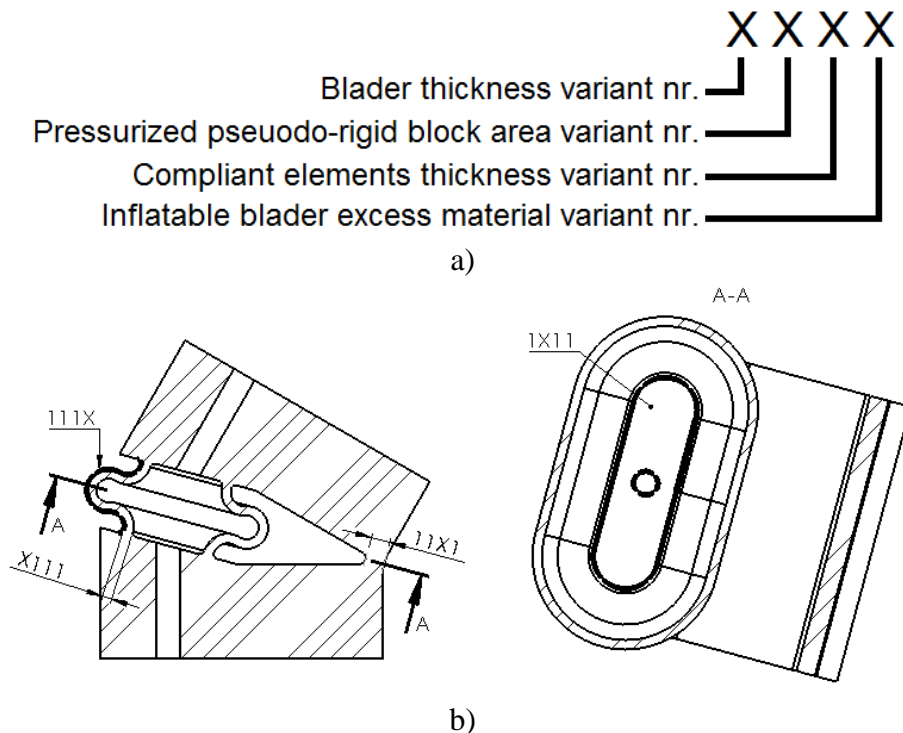


**Fig. 23.** Design variant designation: a) designation chart; b) designated dimensions

The first model (designation: 1111) has been modeled using design 3 for reference and considered baseline for other variations.



## 4.2. Baseline model (variation 1111)

This model has been based on bellow actuated design introduced in subsection 2.2.3. Minor adjustments were introduced in order to geometrically accommodate all the variants planned for this part of the study. The dimensions of variant 1111 can be found in Table 6.

**Table 6.** Dimensional values of variant 1111

Dimension designation				Dimension value of geometry element
x	x	x	x	
1				1 mm
	1			140 mm <sup>2</sup>
		1		2 mm
			1	15 mm

4 model groups (for each design element) have been formed, each with 5 dimensional variants (for each dimension iteration). Only one of the four dimensions has been altered in any given group, this ensures data purity and that model 1111 can be universally used as a starting point in all 4 groups.

Dimension alteration range must be significant to prevent inconclusive observations. It has been decided that approximately 50%-100% change in geometry dimension should display a notable change in joint characteristics if relevant correlation is present.

Variant 1111 was inflated by a pressure of 0.11 MPa (maximum pressure before structural failure) and achieved rotation angle of 12.73° (Fig. 24. a), b)).

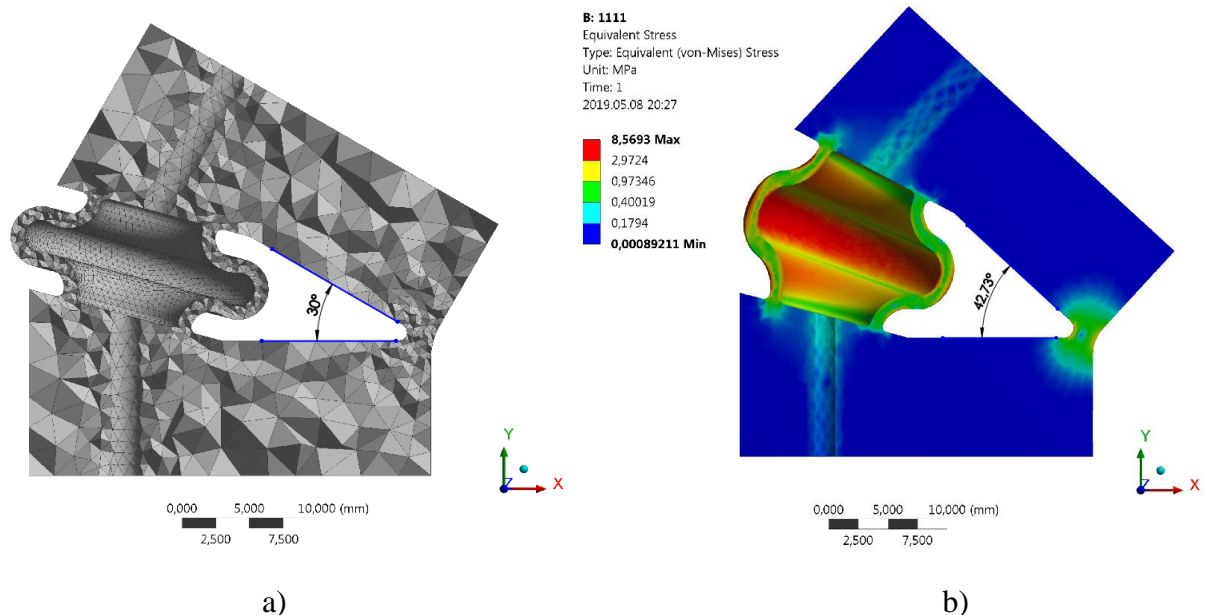
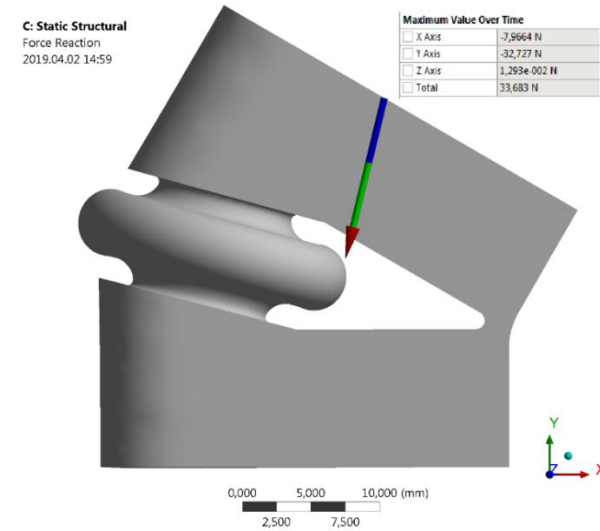
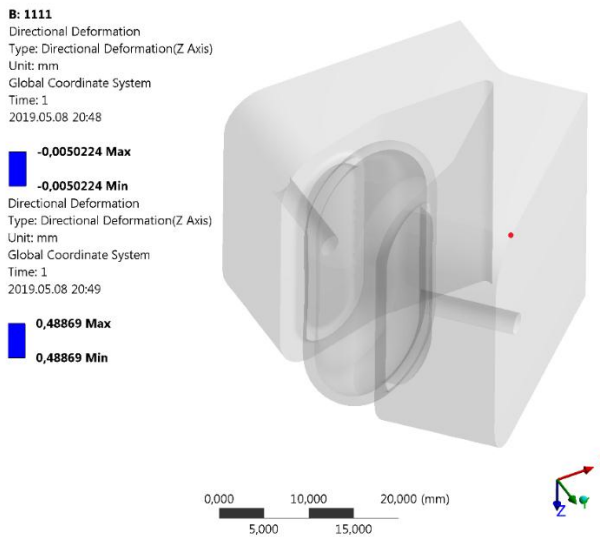


**Fig. 24.** Variant 1111 results: a) joint angle before inflation; b) joint angle after inflation

The actuation produced by pressurized variant 1111 resulted in generated force of 33.68 N (Fig. 25. a)). The external load test revealed a deflection, in the direction of applied force, to be 0.484 mm under the load of 10 N (Fig. 25. b)). These results (Table 7.) have then serve as baseline for determining characteristic improvement or decline and the intensity of said changes.



a)



b)

**Fig. 25.** Variant 1111 results cont.: a) force produced by inflation; b) deformation in z axis before and after external load is applied

**Table 7.** Results of variant 1111

Variant	Angle, °		Force, N	Deflection in z axis, mm		
	Absolute	$\Delta$		Before load	After load	$\Delta$
1111	42.73	12.73	33.683	-0.005	0.489	0.484

### 4.3. Alteration of inflatable bladder thickness (group X111)

The thickness of inflatable actuating element was predicted to be one of the most relevant parameters of the monolithic joint. With increasing thickness, the construct would become more rigid, but also more robust, this, in turn, should result in reduced range of motion, increased actuation force and lower deflection. The relation between bladder thickness and joint parameter has been the focus of this section. Bladder thickness has been increased from 1 mm (same as variant 1111) to 2 mm by intervals of 0.25 mm. All other dimensions have been kept constant. Thickness has been increased by offsetting the external wall of the bladder to avoid changing volume and surface area affected by pressure (Fig. 26.). Resulting data of group X111 testing can be found in Table 8. More raw data for group X111 can be found in Appendix 1.

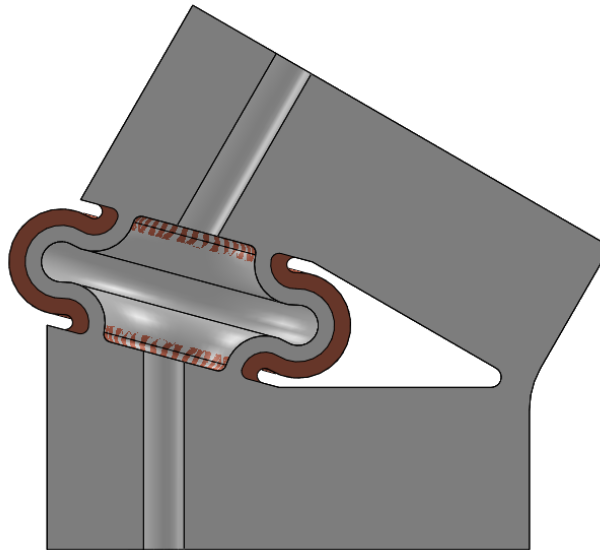


**Fig. 26.** The adjusted bladder thickness as compared to variant 1111

**Table 8.** Results of group X111

Variant	Angle, °		Force, N	Deflection in z axis, mm			Bladder thickness, mm
	Absolute	$\Delta$		Before load	After load	$\Delta$	
1111	42.73	12.73	33.683	-0.005	0.489	0.484	1
2111	40.74	10.74	46.662	-0.009	0.449	0.44	1.25
3111	38.87	8.87	57.763	-0.014	0.404	0.39	1.5
4111	37.6	7.6	70.202	-0.021	0.356	0.335	1.75
5111	36.71	6.71	80.796	-0.025	0.326	0.301	2

These results allow for confirmation of predicted outcomes, but it is the severity of geometry effect on actuation that is the focus of this study. For easier comparison the result differences have been converted into percentage values using variant 1111 results as characteristic baseline (Table 9.).

**Table 9.** Results of group X111 compared in relation to baseline

Variant	Angle		Force		Deflection		Bladder thickness	
	Result, °	Δ, %	Result, N	Δ, %	Result, mm	Δ, %	Dimension, mm	Δ, %
1111	12.73	0.0	33.683	0.0	0.484	0.0	1	0.0
2111	10.74	-15.6	46.662	38.5	0.44	-9.1	1.25	25.0
3111	8.87	-30.3	57.763	71.5	0.39	-19.4	1.5	50.0
4111	7.6	-40.3	70.202	108.4	0.335	-30.8	1.75	75.0
5111	6.71	-47.3	80.796	139.9	0.301	-37.8	2	100.0

It is now clear that all three joint characteristics are heavily affected by bladder thickness. Actuation angle was affected negatively with a maximum decrease of 47.3%. Conversely, joint deflection has been reduced by 37.8% from baseline model. Most notably the produced force displays a strong positive relation to thickness, reaching up to 139.9% improvement. While these numbers clearly show which characteristics are more affected by bladder thickness within the tested range, graphic representation and trend functions are more informative and can be found in Fig. 27.

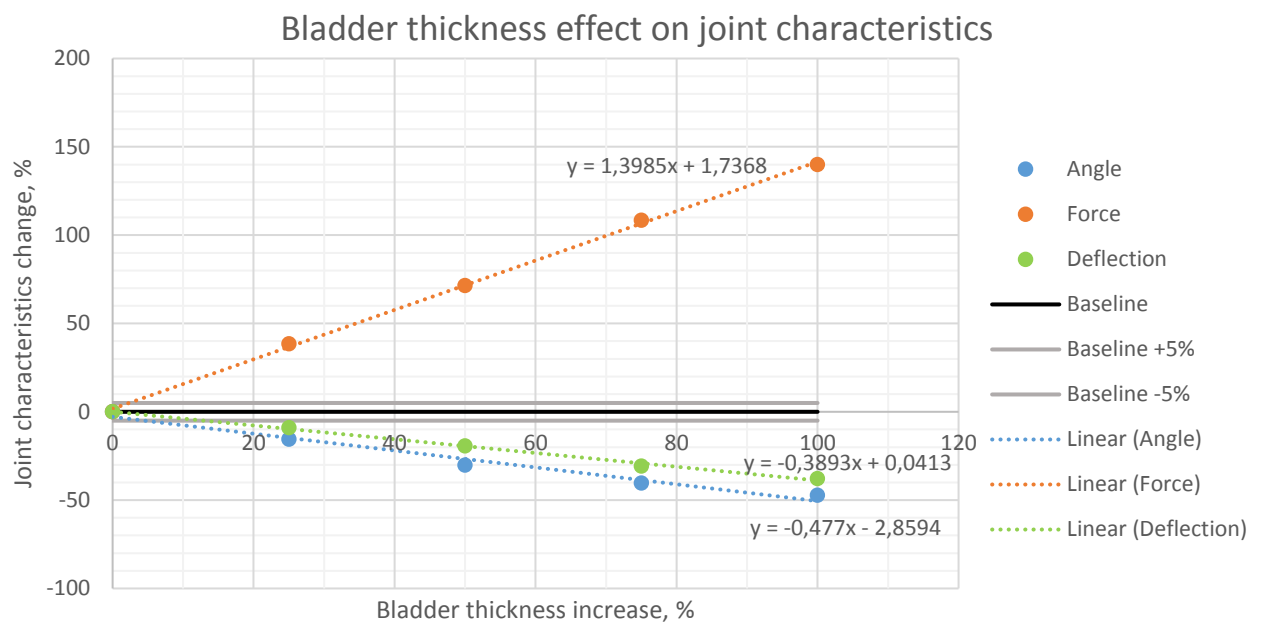


**Fig. 27.** Bladder thickness effect on joint characteristics along with trendlines and their functions

Threshold lines were added at  $\pm 5\%$  chart marks. If the maximum tested dimension change does not cause a joint characteristic to exceed the  $\pm 5\%$  marks, characteristic may be considered unaffected by geometry element. This is a precautionary measure placed to avoid inconclusive data. FEA can introduce minor deviations even when testing nearly identical conventional designs. A compliant design is even more susceptible due to function related and unrelated elements not being clearly separated.

#### 4.4. Alteration of pseudo-rigid block area affected by pressure (group 1X11)

If area (and, in turn, perimeter) connecting the bladder and pseudo-rigid blocks may be reduced without negative impact on performance, it would allow for more compact designs. This would

further reduce overall size while possibly increasing stroke and force while allowing for greater freedom when positioning the bladder within the joint. The geometry impact on produced force was the main concern for this test. No major changes in actuation angle or deflection were expected. Surface area shared by the bladder and one of the blocks has been reduced from 140 mm<sup>2</sup> (same as variant 1111) to 60 mm<sup>2</sup> by intervals of 20 mm<sup>2</sup>. All other dimensions have been kept constant. Alteration illustrated in Fig. 28. Resulting data of group 1X11 testing can be found in Table 10. More raw data for group 1X11 can be found in Appendix 2. Graphical representation of the results and relevant trend functions can be seen in Fig. 29.

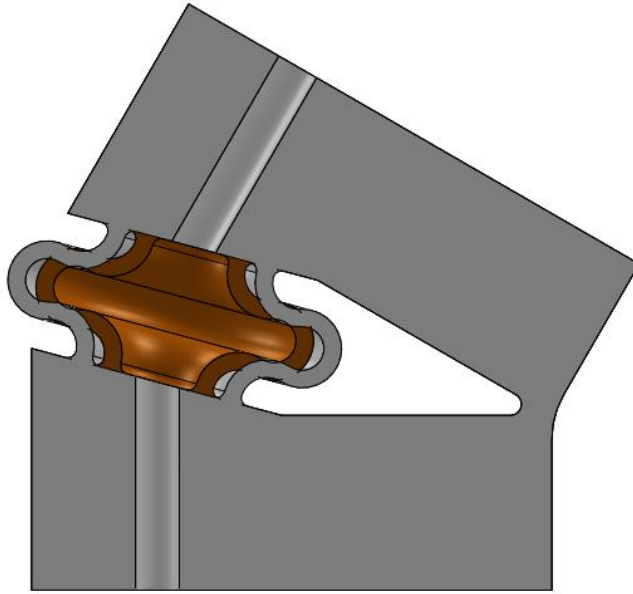


**Fig. 28.** The adjusted pseudo-rigid block area affected by pressure as compared to variant 1111

**Table 10.** Results of group 1X11 compared in relation to baseline

Variant	Angle		Force		Deflection		Pressurized pseudo-rigid block area	
	Result, °	Δ, %	Result, N	Δ, %	Result, mm	Δ, %	Dimension, mm <sup>2</sup>	Δ, %
1111	12.73	0.0	33.683	0.0	0.484	0.0	140	0.0
1211	12.95	1.7	33.154	-1.6	0.485	0.2	120	-14.3
1311	12.94	1.6	32.132	-4.6	0.495	2.3	100	-28.6
1411	12.99	2.0	31.124	-7.6	0.502	3.7	80	-42.9
1511	12.81	0.6	29.519	-12.4	0.504	4.1	60	-57.1

## Pressurized pseudo-rigid block area effect on joint characteristics

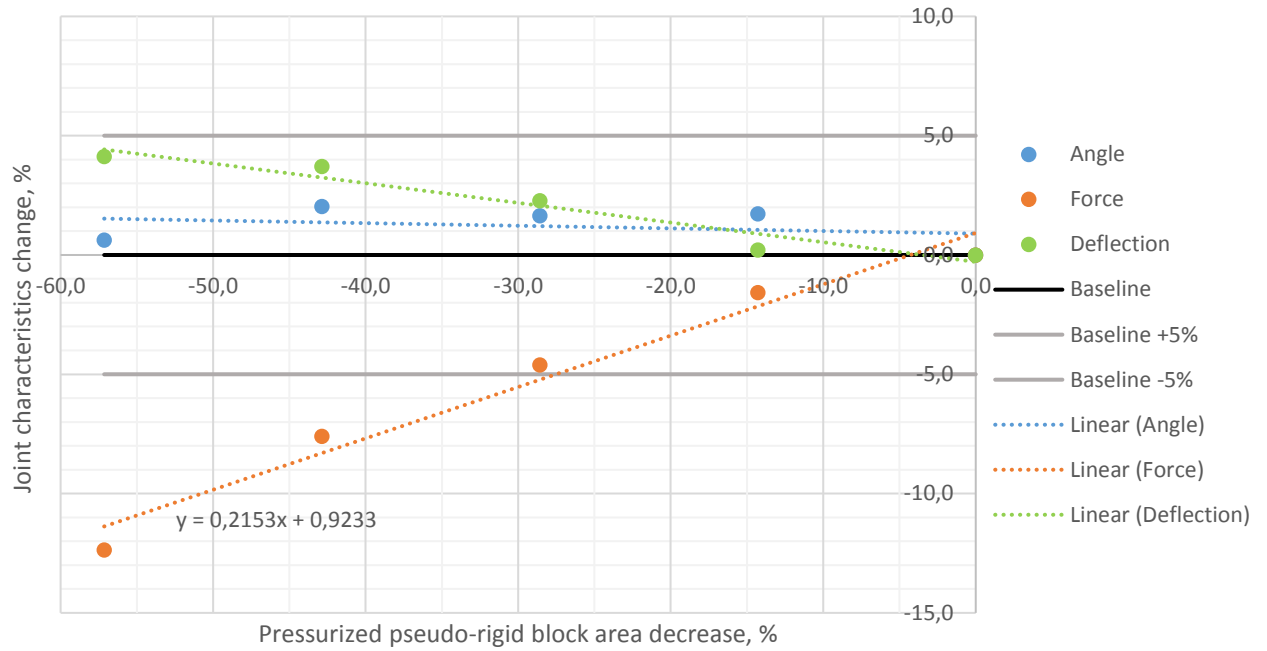


**Fig. 29.** Pressurized pseudo-rigid block area effect on joint characteristics along with threndlines and their functions

Geometrical element effects on actuation angle and joint deflection were proven negligible. Only minor decrease in actuation force was observed, likely caused by overall decrease of pressurized surface.

### 4.5. Alteration of compliant element thickness (group 11X1)

The compliant element of monolithic joint presented in this study is an essential part of the design regardless of iteration. It directs motion, constrains degrees of freedom, provides rigidity and is largely responsible for joints return to primary position upon deflation. Its effectiveness as a return mechanism is described by its rigidity which, without sacrificing accuracy, can be adjusted by changing its minimum thickness. In this group compliant element thickness has been increased from 2 mm (same as variant 1111) to 4 mm by intervals of 0.5 mm. All other dimensions have been kept constant. A decrease in deflection and actuation angle was expected. No major changes to produced force was expected. Alteration illustrated in Fig. 30. Resulting data of group 11X1 testing can be found in Table 11. More raw data for group 11X1 can be found in Appendix 3. Graphical representation of the results and relevant trend functions can be seen in Fig. 31.

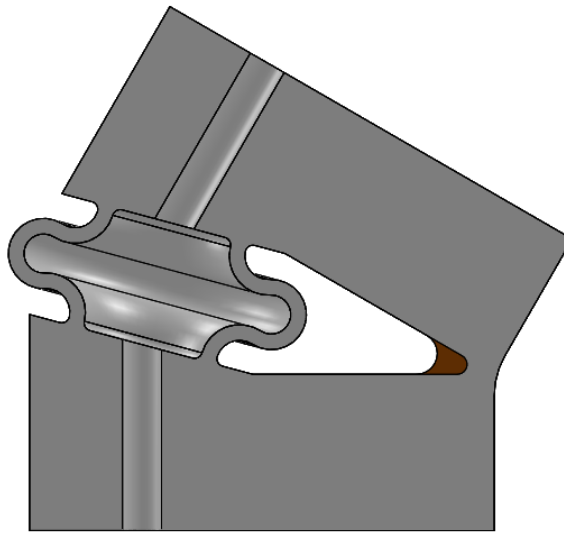


**Fig. 30.** The adjusted compliant element thickness as compared to variant 1111

**Table 11.** Results of group 11X1 compared in relation to baseline

Variant	Angle		Force		Deflection		Compliant element thickness	
	Result, °	Δ, %	Result, N	Δ, %	Result, mm	Δ, %	Dimension, mm	Δ, %
1111	12.73	0.0	33.683	0.0	0.484	0.0	2	0.0
1121	13.32	4.6	35.682	5.9	0.45	-7.0	2.5	25.0
1131	12.86	1.0	36.132	7.3	0.405	-16.3	3	50.0
1141	12.63	-0.8	37.14	10.3	0.393	-18.8	3.5	75.0
1151	12.82	0.7	39.283	16.6	0.367	-24.2	4	100.0

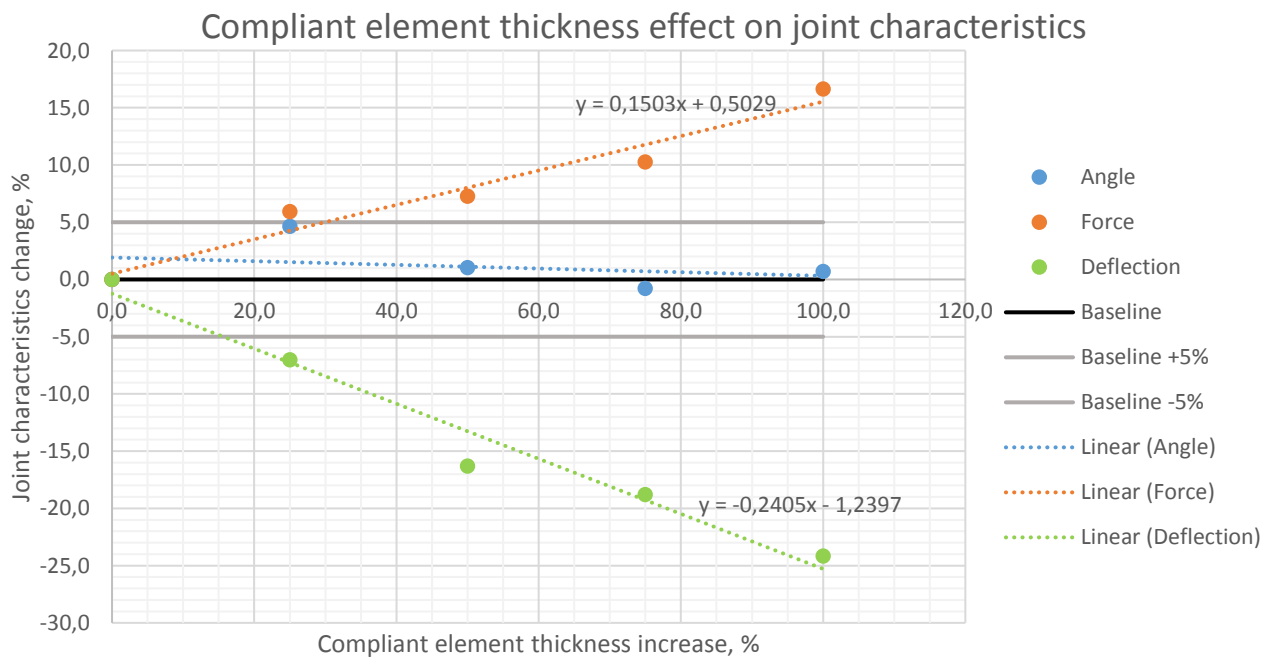


**Fig. 31.** Compliant element thickness effect on joint characteristics along with trendlines and their functions

A minor decrease in deflection was observed. Effect on actuation angle was negligible and seemingly random, it likely originates from errors in calculation and measurements. A minor increase in produced force was calculated.

#### 4.6. Alteration of inflatable bladder material excess (group 111X)

Pressurized surface area is one of the major factors when considering fluid actuators. Group 1X11 tests proved that changing the rigid part of the bladder has minor effect on produced force. Tests in this chapter had involved increasing the amount of surface area available for expansion. This has been regulated by the length of bellow profile as seen in the joint cross section (Fig. 32.). Length of the profile has been increased from 15 mm (same as variant 1111) to 21 mm by intervals of 1.5 mm. All other dimensions have been kept constant. Improvement of actuation angle was expected, effect on produced force and deflection was unclear. Resulting data of group 111X testing can be found in Table 12. More raw data for group 111X can be found in Appendix 4. Graphical representation of the results and relevant trend functions can be seen in Fig. 33.

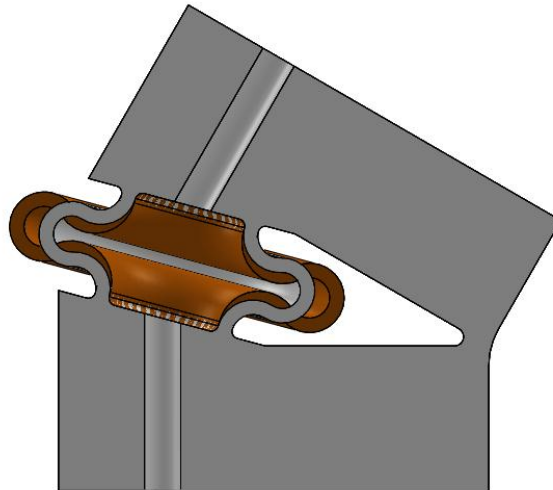


**Fig. 32.** The adjusted bladder profile length as compared to variant 1111

**Table 12.** Results of group 111X compared in relation to baseline

Variant	Angle		Force		Deflection		Bladder profile length	
	Result, °	$\Delta$ , %	Result, N	$\Delta$ , %	Result, mm	$\Delta$ , %	Dimension, mm	$\Delta$ , %
1111	12.73	0.0	33.683	0.0	0.484	0.0	15	0.0
1112	15.27	20.0	31.717	-5.8	0.496	2.5	16.5	10.0
1113	18.01	41.5	31.242	-7.2	0.508	5.0	18	20.0
1114	19.58	53.8	29.385	-12.8	0.507	4.8	19.5	30.0
1115	21.93	72.3	29.37	-12.8	0.511	5.6	21	40.0



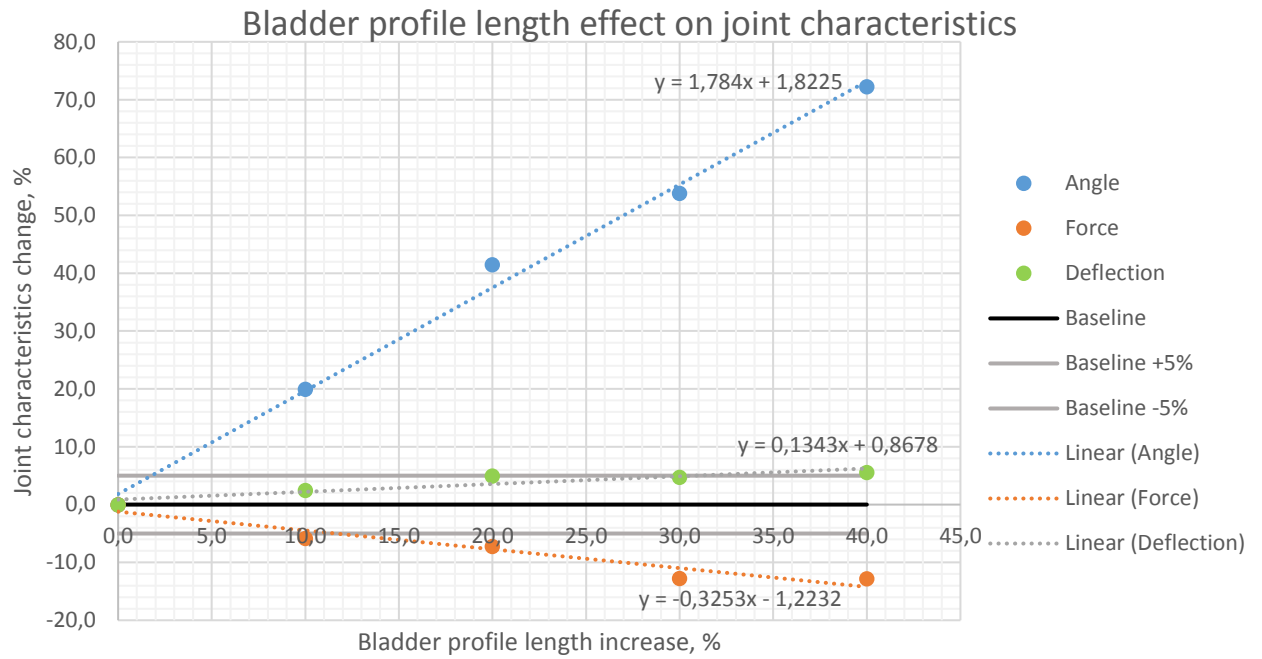


**Fig. 33.** Bladder profile length effect on joint characteristics along with threndlines and their functions

Increasing the bladder profile has produced the most significant actuation angle changes out of all testing groups. In addition, the negative effects on joint force and deflection were minor. Geometry of the bladder is the most complex aspect of the monolithic joint and most demanding in terms of space. However, this is the only geometric element that has produced considerable improvement to the range of motion and will likely be important when optimizing the design.

#### 4.7. Evaluation of geometric elements and design optimization

With the data gathered during previous tests it becomes clear, that some alterations can substantially improve aspects of the initial design without significant drawbacks. Additionally, it provides a better understanding of designs overall capabilities. For example, after such extensive geometry variations, it has become clear that designs reach ultimate stress not due to bladder pressure, but the severity of deformation. This implies that joints may be capable of even higher force output if resistance is encountered early in the motion.

In terms of geometry variations, the ones presented in this study were parametrically defined, but there are likely considerable improvements to be made using more freeform designs. Information gathered here should be useful regardless. The approximate effect of geometric elements on joint characteristics have been summarized in Table 13.

**Table 13.** Summary of geometry-performance relations found during testing

Geometric element	Affected characteristic	Approximate affect relation	Correlation
Bladder thickness (group X111)	Angle	-0.48:1	Major direct correlation
	Force	1.4:1	Major inverse correlation
	Deflection	-0.39:1	Major inverse correlation
Pressurized pseudo-rigid block area (group 1X111)	Angle	n/a	No correlation
	Force	0.22:1	Minor direct correlation
	Deflection	n/a	No correlation
Compliant element thickness (group 11X1)	Angle	n/a	No correlation
	Force	0.15:1	Minor direct correlation
	Deflection	-0.24:1	Major inverse correlation
Bladder profile length (group 111X)	Angle	1.78:1	Major direct correlation
	Force	-0.33:1	Major inverse correlation
	Deflection	0.13:1	Minor direct correlation

Combining the individual elements into a singular design should allow for an optimal design to be made. This design would likely not excel in any specific characteristic, but it would be an objective improvement over the baseline variant 1111. In order to determine which variations provide the most benefit with least drawbacks a simple scoring system will be implemented. Result difference percentages will be used as point values to calculate an overall benefit score (OBS) (Table 14.). Angle and produced force values will be added and the deflection value subtracted (it is a negative characteristic). It should be noted that this evaluation presumes that relative improvements in angle, force of deflection are all equally important.

$$OBS = Angle + Force - Deflection$$

**Table 14.** Benefit summary across all tested variants (the most beneficial variations were marked in yellow, least beneficial – in grey)

Variant	Benefit values			
	Angle	Force	Deflection	OBS
1111	0.0	0.0	0.0	0.0
2111	-15.6	38.5	-9.1	32.0
3111	-30.3	71.5	-19.4	60.6
4111	-40.3	108.4	-30.8	98.9
5111	-47.3	139.9	-37.8	130.4
1111	0.0	0.0	0.0	0.00
1211	1.7	-1.6	0.2	-0.05
1311	1.6	-4.6	2.3	-5.2
1411	2.0	-7.6	3.7	-9.3
1511	0.6	-12.4	4.1	-15.9
1111	0.0	0.0	0.0	0.0
1121	4.6	5.9	-7.0	17.6
1131	1.0	7.3	-16.3	24.6
1141	-0.8	10.3	-18.8	28.3
1151	0.7	16.6	-24.2	41.5
1111	0.0	0.0	0.0	0.0
1112	20.0	-5.8	2.5	11.6
1113	41.5	-7.2	5.0	29.3
1114	53.8	-12.8	4.8	36.3
1115	72.3	-12.8	5.6	53.9

With the most advantageous variations identified, they can be combined into an optimal variation - 5155. However, the large dimensions comprising this variant make it geometrically invalid. As such, a compromise was made. The 1X11 group appears to have the lowest overall impact on performance. With that in mind the 5555 variant will provide a valid substitute (Fig. 34.). The combined design has gone through the same testing process and the results can be seen in Table 15.

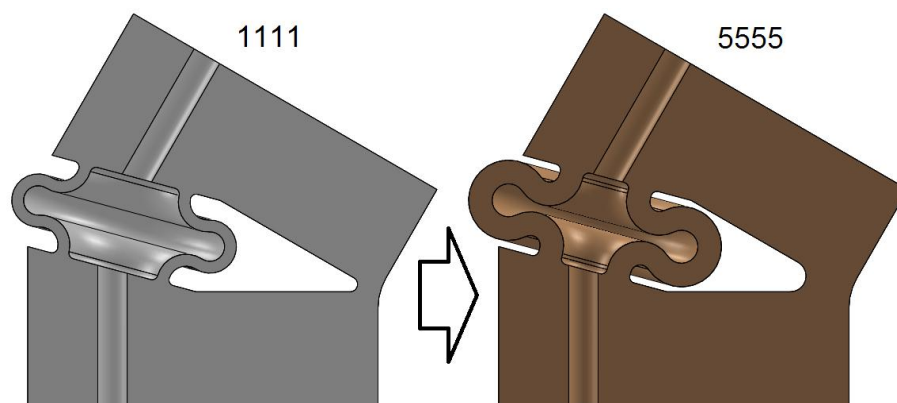


**Fig. 34.** Optimized variant 5555 as compared to variant 1111

**Table 15.** Results of combination variant 5555

Variant	Angle, °		Force, N	Deflection in z axis, mm		
	Absolute	$\Delta$		Before load	After load	$\Delta$
5555	41.75	11.75	68.996	-0.029	0.331	0.302

Comparing the benefit values between previously highest scoring variant 5111 and optimized variant 5555 the improvement appears miniscule. However, upon closer inspection the optimized variant sacrifices some of variants 5111 excessive force in order to minimize the actuation angle penalty while maintaining reduced deflection (Table 16.).

**Table 16.** Benefit comparison between baseline, highest individual and combination variants

Variant	Benefit values			
	Angle	Force	Deflection	OBS
1111	0	0	0	0
5111	-47.3	139.9	-37.8	130.4
5555	-7.7	104.8	-37.6	134.7

In addition to optimization, the data can also be used to create specialized models. For example, the highest actuation angle would be achieved with variant 1425 (Fig. 35.), highest force with variant 5151 (Fig. 35.) and lowest deflection with 5151 (Fig. 35.).

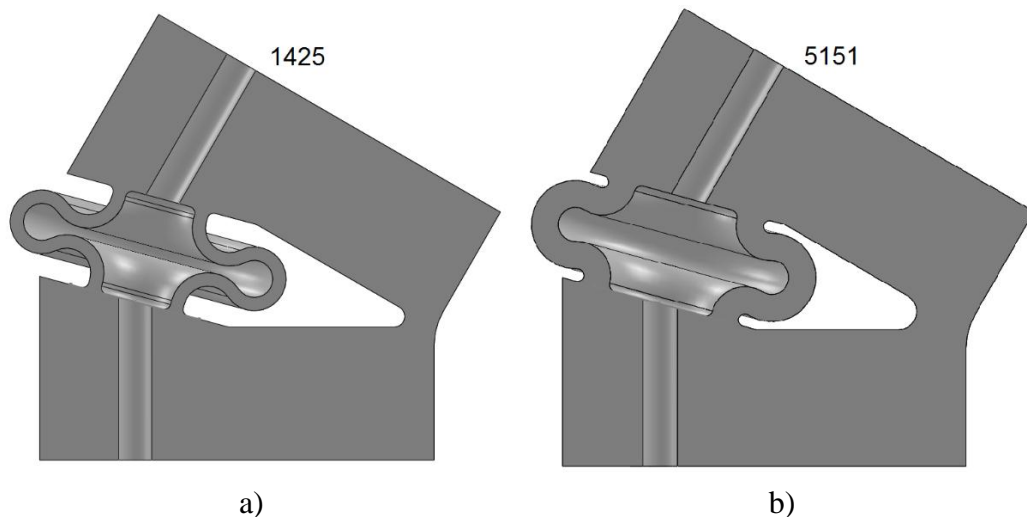


**Fig. 35.** Specialized combinations: a) actuation angle optimization; b) force and deflection optimization

With the completion of the comparative part of the study, and the experience and data gained through it, a more streamlined model of the compliant pressure actuated monolithic joint has been created (Fig. 36.). This model contains geometric elements of variant 5155 and will be the final joint presented in this study.

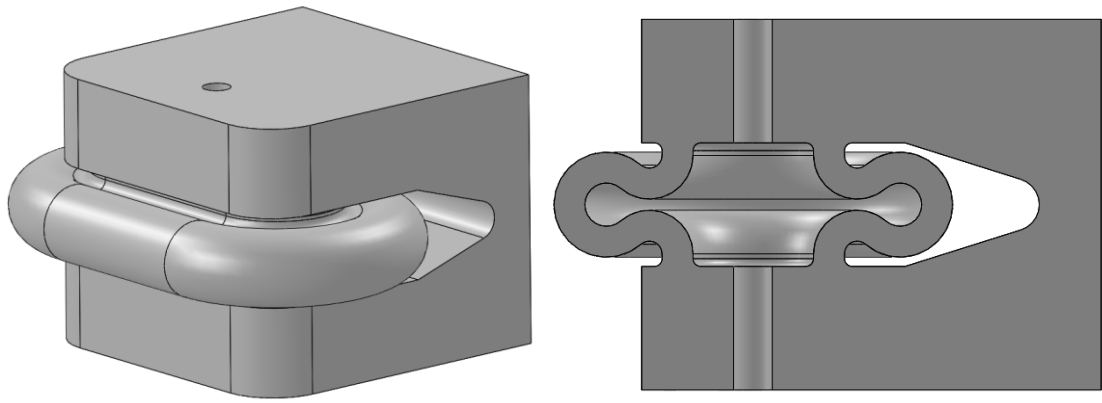


**Fig. 36.** Combination 5155 with minor design revisions

The final design was analogically tested (Table 17.) and, as expected, shows considerable performance improvements even when compared with the 5555 variant (Table 18.). It should be noted that due to changes in design, not included in the comparative study, these results can only serve as a frame of reference.

**Table 17.** Results of revised combination variant 5155

Variant	Angle, °	Force, N	Deflection in z axis, mm		
	$\Delta$		Before load	After load	$\Delta$
5155_Revised	12.29	82.014	-0.053	0.26	0.207

**Table 18.** Benefit comparison between baseline, highest individual, combination 5555 and revised 5155 variants

Variant	Benefit values			
	Angle	Force	Deflection	OBS
1111	0	0	0	0
5111	-47.3	139.9	-37.8	130.4
5555	-7.7	104.8	-37.6	134.7
5155_Revised	-3.5	143.5	-57.2	197.3

The data acquired in this study has allowed for design optimization and prediction within the tested range. However, the geometry-performance relation trends observed in this study (Table 13.) are expected to be scalable, similarly to compliant mechanisms themselves and can be regarded as guide lines for designing similar monolithic joints.

## **5. Joint powering, control and application recommendations**

While the effectiveness of compliant pressure actuated monolithic joints has been established, the question of their compatibility with existing technologies remain. In this chapter suggestions regarding powering and control of this new actuator have been presented. Additionally, recommendations for possible application have been made.

### **5.1. Powering the monolithic joint**

All pressure actuators rely on fluid to function. This fluid most commonly comes either in a form of gas (e.g. air, carbon dioxide) or liquid (e.g. oil, emulsion). Hydraulic and pneumatic cylinders are primary examples of pressure actuators. While pneumatic and hydraulic actuators may both use fluids, they are not interchangeable. This is primarily due to vast differences in construction and application. A hydraulic actuator must sustain higher pressures, is self-lubricating (which may contaminate its environment) and uses seal suitable to isolate liquid while pneumatic seals isolate gasses. The joints presented in this study have no risk of fluid contamination (structural failure not withstanding) and do not use any seals due to their inflatable nature. Therefore, if the requires low pressure can be maintained, any fluid is applicable.

If actuating speed is not important pressure can also be achieved by thermal expansion. Paraffin wax is already used for actuations for its expansion ration and low melting temperature [16]. It could be used in the actuators presented in this study making them applicable in the same ways and more due to flexibility of additively manufactured designs. With the melting point of TPU [10] far exceeding that of paraffin, a monolithic joint, with wax injected directly into the inflating bladder, could be placed in the varying temperature environment and operate autonomously.

### **5.2. Monolithic joint control**

When considering the control of these joints three values must be monitored: pressure, actuation angle and, optionally, temperature (if thermo expansion is applied). As the fluid would be pumped into the joint in a conventional way, conventional system pressure measurement methods would apply. Actuation angle, however, is specific to the joint construction and requires a specific solution.

Capacitive proximity sensors would be a viable solution, but as standard capacitive sensors have their component integrated into a single unit, the final product becomes too massive to be integrated into designs considered in this study [17]. A specialized capacitive sensor with its electrodes attached to the joint and other components removed further from the joint would make it applicable, but inclusion of such non-standard sensor would inflate the production cost.

As the designs take up a nonconventional position scale-wise (too large for MEMS yet too small for conventional equipment), size if a major factor when choosing a sensor. Considering this limitation, Hall proximity sensors are recommended (Fig. 37.). While they have limited detection range, losing effectiveness after more than 10 mm [18], it falls within the motion range created by the actuator. Small size is not the only convenience provided by using a Hall sensor. As there is no reason these monolithic joints could not be used in contaminated environment without regular maintenance, they could operate covered in dirt. A Hall sensor relies on a permanent magnet as a point of reference rather than material surrounding it and, in this case, may prove more reliable than a capacitive sensor.



**Fig. 37.** A Hall sensor size comparison [18]

As placement of a standard part within the custom joint becomes inevitable, questions of fixation present themselves. The flexible material used to make the joint provides a unique opportunity for assembly based around interference and snap fits (Fig. 38.). Especially since the pseudo-rigid blocks have displayed negligible strain during actuation (Fig. 39.).

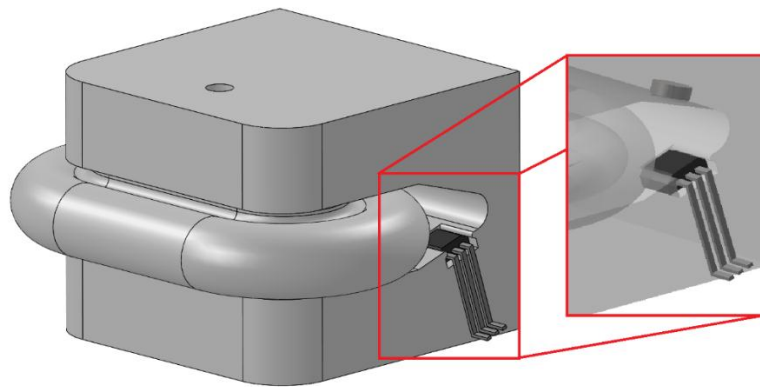


**Fig. 38.** Monolithic, actuated joint with Hall sensor and a neodymium magnet snap fitted into place

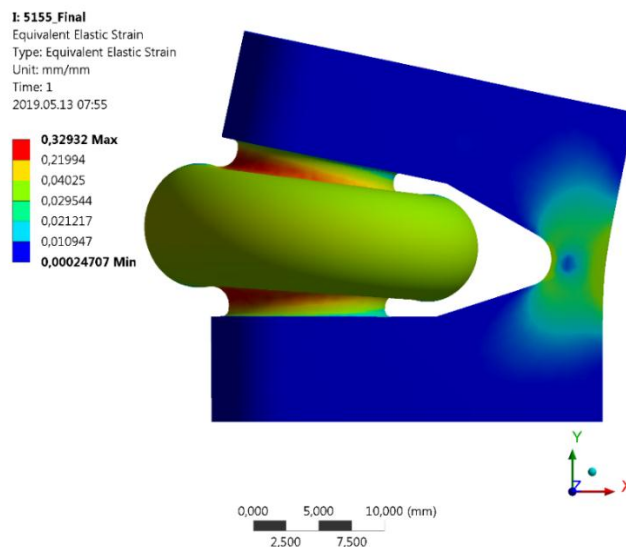


**Fig. 39.** Strain propagation through the pseudo-rigid blocks

Due to angular motion of the joint, the permanent magnet, in relation to the sensor, would move in a complex manner. This would include moving away in two axes while also rotating (Fig. 40.).

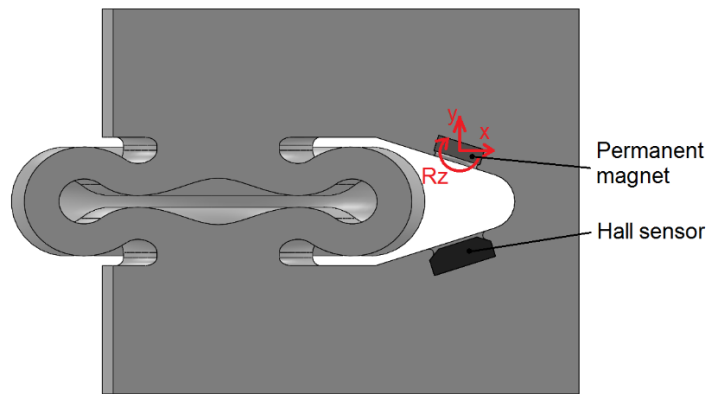


**Fig. 40.** Permanent magnet motion in relation to sensor

For this reason, the sensor voltage output would not correlate linearly to actuation angle. However, calibrating the sensor system for this motion would solve this problem. Calibration would be done by setting the joint to known angles and plotting them to sensor voltage outputs.

### 5.3. Recommendations

While this study was started under the premise of developing a mechanism that would bridge the accuracy gap between conventional and soft robotics, it has become clear that these joints are more suitable for another application. The motion and force produced, while minor by industrial actuator standards, is an order of magnitude higher than that provided by micro electromechanical systems. And with compliant mechanics scalability, designs like these could fill the scale gap.

Most prominent tasks for these devices would be adjustment and regulation. As previously mentioned, these joints could work similarly to wax actuators and regulate thermal systems (e.g. water heating systems, greenhouse ventilation etc.) (Fig. 41.).



**Fig. 41.** Autonomous thermoactuator used to control greenhouse ventilation [19]

Preexisting, previously manually operated, systems could be easily upgraded with these joints, as the mechanism and fixation can be customized for a specific application without inflating the production cost (Fig. 42.).



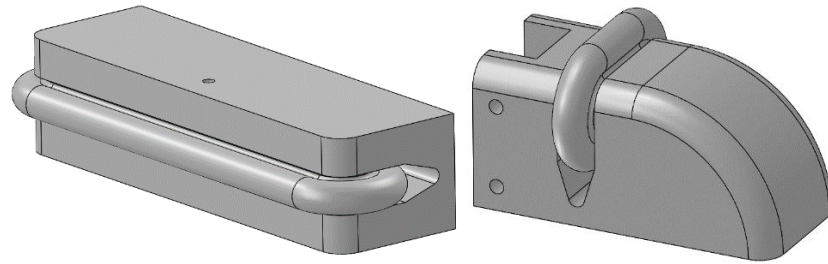


**Fig. 42.** Monolithic, actuated joints customized for specific applications

The designs can also be used in less primitive ways. The joints could operate as accurate adjustment mechanisms even with a high mass object affixed to them. The accuracy and applicability can be improved with additional inflating bladders, making the joint differential (Fig. 43.). As preload was not investigated in this study it is possible that differential configurations could also double the actuation angle.

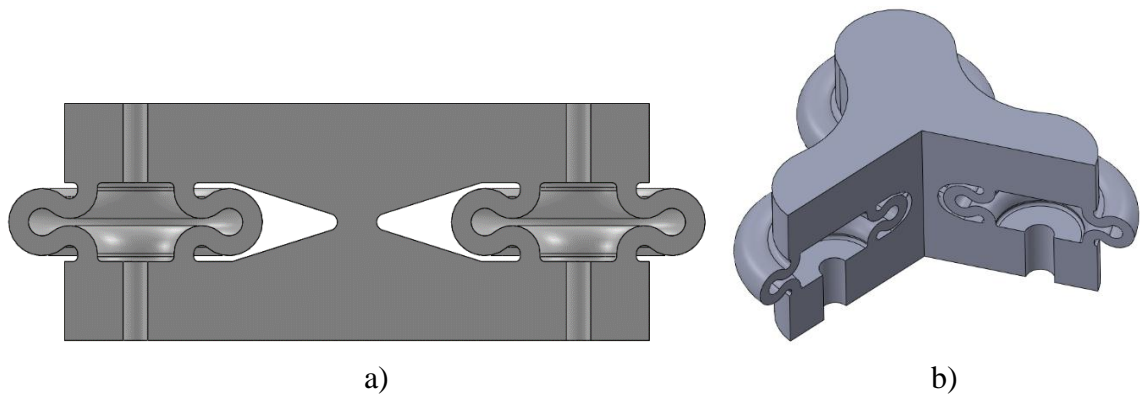


**Fig. 43.** Differential, monolithic, actuated joints: a) pivoting variation; b) omnidirectional variation

These designs could direct optical beams by redirecting the source device or level objects considerably more massive than the device itself. Additionally, the joint would still be lighter and smaller than the alternatives (Fig. 44.).

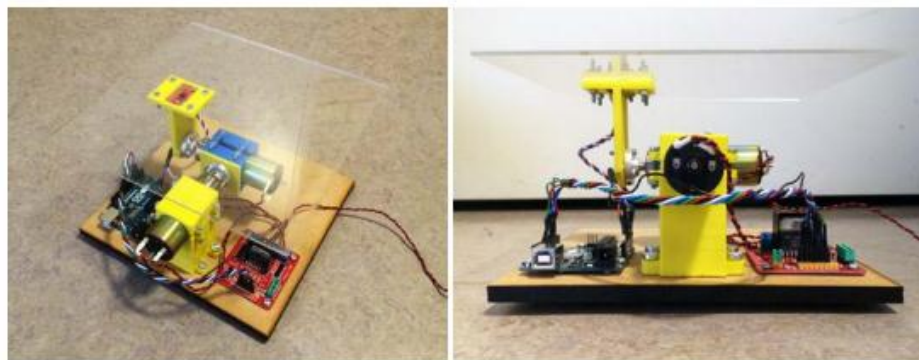


**Fig. 44.** Stabilizing platform using two electric motors [20]

Above all, designs presented in this study should be used as a jumping of point when designing more complex monolithic mechanisms.

## Conclusion

It was the purpose of this study was to investigate the viability of monolithic, actuated joint. This process has been divided into several stages. First the concept had to be proven valid by having motion, force and maintaining rigidity. Then, since geometry is the only resource available, its influence on performance had to be documented. This would prove the possibility of designing the actuated joint in accordance to performance requirements – a crucial aspect for any actuator. Finally, the developed designs had to be considered in relation to existing technologies.

1. 9 combinations of geometry and material were established. Materials of 3 vastly different flexibilities were proposed and combined with 3 geometries inspired by existing soft robotics. After 4 virtual simulations only the most rigid material (~55% elongation) was proven effective and only 2 geometries produced viable results with a bellow-based design outperforming the corrugated design by having double the actuation angle (~14.5°). The bellow design was then used for the next stage of the investigation.
2. After systematically altering the dimensions of vital bellow design geometric elements, correlations to performance have been observed. This establishes that monolithic, actuated joints can be designed with specific performance in mind only by alterations to few aspects of geometry in a predictable manner. Inflatable bladder thickness was proven most responsive with the 1.4:1 affect ratio on actuator force, -0.48:1 on actuation angle and -0.39:1 on joint deflection. Bladder profile length proved similarly influential with a 1.78:1 affect ratio on actuation angle and a -0.33:1 relation to force. Compliant element thickness showed minor effect on joint force and deflection. Bellow perimeter was proven almost inert only having minor impact on force. With this information, a joint could be designed with specific application, surroundings and fixation in mind and then brought up to performance specifications without extensive testing.
3. The designs could be powered by any pressurized fluid and, due to low actuation stroke, even by means of thermal expansion. For actuation angle tracking a Hall sensor in combination with a permanent magnet would be applicable. Joints minimalistic motion makes it most appropriate for adjustment and regulation tasks, making them comparable to thermoactuators in terms of performance, but more discreet, versatile and flexible in terms of design.

## List of references

1. MALONEY, J. M. *3-D Microfabrication* [online]. 2001 [viewed 15 February 2018]. Available from: [http://john.maloney.org/3d\\_microfab.htm](http://john.maloney.org/3d_microfab.htm)
2. BAPAT, S. G. *On the design and analysis of compliant mechanisms using the pseudo-rigid-body model concept*. Doctoral dissertation, Missouri University of Science and Technology, 2015.
3. HOWELL, L. L. *Compliant mechanisms*. New York: John Wiley & Sons, 2001. ISBN 0-471-38478-X.
4. BALASUBRAMANIAN, R and M. A. DOLLAR. *A Comparison of Workspace and Force Capabilities between Classes of Underactuated Mechanisms*. Shanghai, China, 2011. IEEE.
5. GORISSEN, B. et al. Elastic Inflatable Actuators for Soft Robotic Applications. *Advanced Materials* [online]. 2017, **29**(43) [viewed 17 February 2018]. Available from: doi:10.1002/adma.201604977.
6. TUDELFT. *3D Printing Soft Robotics* [online]. 2015 [viewed 17 February 2018]. Available from: <https://softrobotics2015.weblog.tudelft.nl/>
7. FORMLABS. *Material Data Sheet* [online]. 2018 [viewed 9 March 2019]. Available from: <https://formlabs-media.formlabs.com/datasheets/XL-DataSheet-601.pdf>
8. STRATASYS. *PolyJet Material Data Sheet* [online]. 2016 [viewed 9 March 2019]. Available from: [http://usglobalimages.stratasys.com/Main/Files/Material\\_Spec\\_Sheets/MSS\\_PJ\\_PJMaterialsDataSheet.pdf?v=635785205440671440](http://usglobalimages.stratasys.com/Main/Files/Material_Spec_Sheets/MSS_PJ_PJMaterialsDataSheet.pdf?v=635785205440671440)
9. BLANES, C., M. MELLADO, and P. BELTRAN. Novel Additive Manufacturing Pneumatic Actuators and Mechanisms for Food Handling Grippers. *Actuators* [online]. 2014, **3**(3), 205-225 [viewed 24 February 2018]. Available from: doi:10.3390/act3030205.
10. ULTIMAKER. *Technical Data Sheet TPU 95A* [online]. 2018 [viewed 5 October 2018]. Available from: <https://ultimaker.com/download/74605/UM180821%20TDS%20TPU%2095A%20RB%20V10.pdf>
11. WOHLERS ASSOCIATES. Wohlers Report 2010: 3D Printing and Additive Manufacturing State of the Industry. *Wohlers Report*. 2010. ISBN 0-9754429-6-1.
12. DONG, L., L. DONG, and R. S. LAKES. A unit cell structure with tunable Poisson's ratio from positive to negative. *Material Letters*. 2016, **164**, 456-459 [viewed 5 October 2018] Available from: doi:10.1016/j.matlet.2015.11.037.
13. SLESARENKO, V. and S. RUDYKH. Towards mechanical characterization of soft digital materials for multimaterial 3D-printing. *International Journal of Engineering Science*. 2018, **123**, 62-72 [viewed 6 October 2018]. Available from: doi:10.1016/j.ijengsci.2017.11.011.
14. QI, H. J. and M. C. BOYCE. Stress-Strain Behavior of Thermoplastic Polyurethane. *Mechanics of Material*. 2005, **37**(8), 817-839 [viewed 10 October 2018]. Available from: doi:10.1016/j.mechmat.2004.08.001
15. GAISER, I. et al. Compliant Robotics and Automation with Flexible Fluidic Actuators and Inflatable Structures. *IntechOpen*. 2012 [viewed 10 November 2018]. Available from: doi:10.5772/51866

16. OGDEN, S. et.al. Review on miniaturized paraffin phase change actuators, valves, and pumps. *Microfluid Nanofluid.* 2014, **17**, 53-71 [viewed 18 March 2019]. Available from: doi:10.1007/s10404-013-1289-3
17. AUTOMATION MEDIA. *Capacitive Proximity Sensors Theory of Operation* [online]. 2019 [viewed 22 March 2019]. Available from: [http://www.automationmedia.com/Port1050/SiemensFreeCourses/snrs\\_4.pdf](http://www.automationmedia.com/Port1050/SiemensFreeCourses/snrs_4.pdf)
18. JAZNY, J. and M. ČURILLA. Position Measurement with Hall Effect Sensors. *American Journal of Mechanical Engineering.* 2013, **1**(7), 231-235 [viewed 22 March 2019]. Available from: doi:10.12691/ajme-1-7-16.
19. STPAULSGARWOOD. *Greenhouse Automatic Vents* [online]. 2018 [viewed 25 March 2019]. Available from: <https://www.stpaulsgarwood.com/greenhouse-automatic-vents.html>
20. NORDLOF, J. and P. LAGUSSON. *Self-Stabilizing Platform: How To Compensate For Imbalance With Feedback From An IMU.* Bachelor's thesis, KTH Royal Institute of Technology, 2015.

## Appendices

### Appendix 1. Alteration of inflatable bladder thickness (group X111) results

**Table 19.** Variant 2111 results

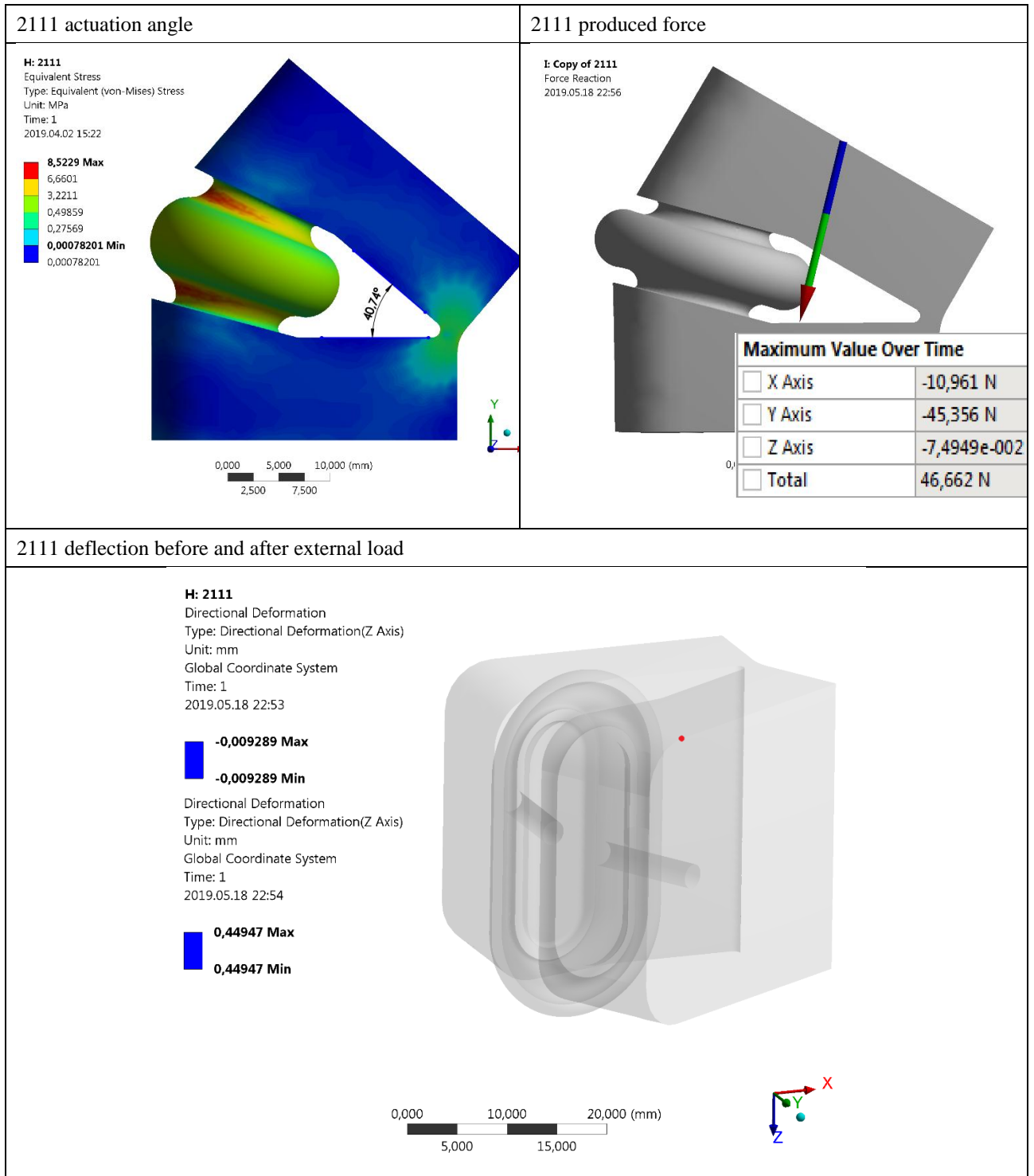


**Table 20.** Variant 3111 results

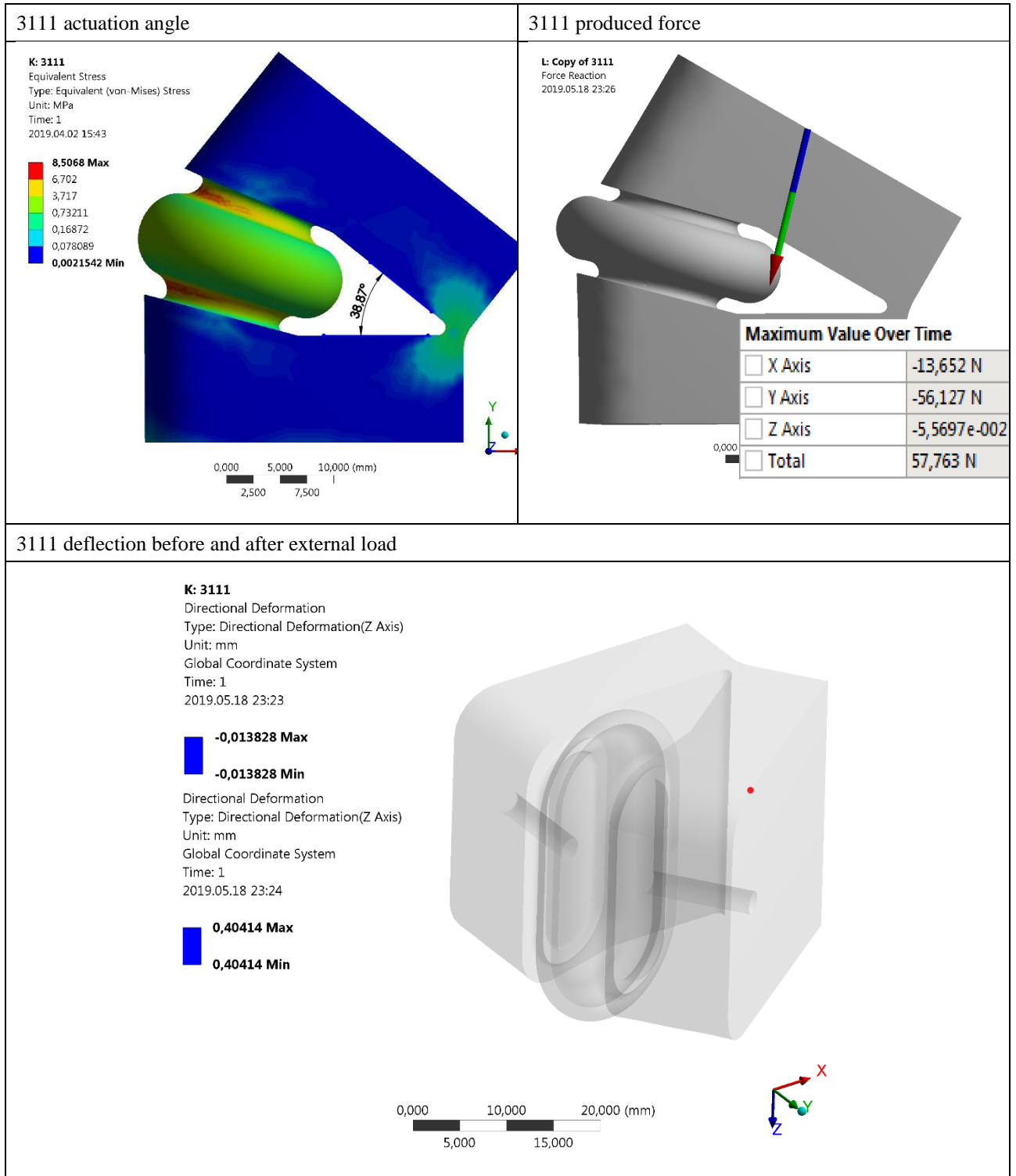


**Table 21.** Variant 4111 results

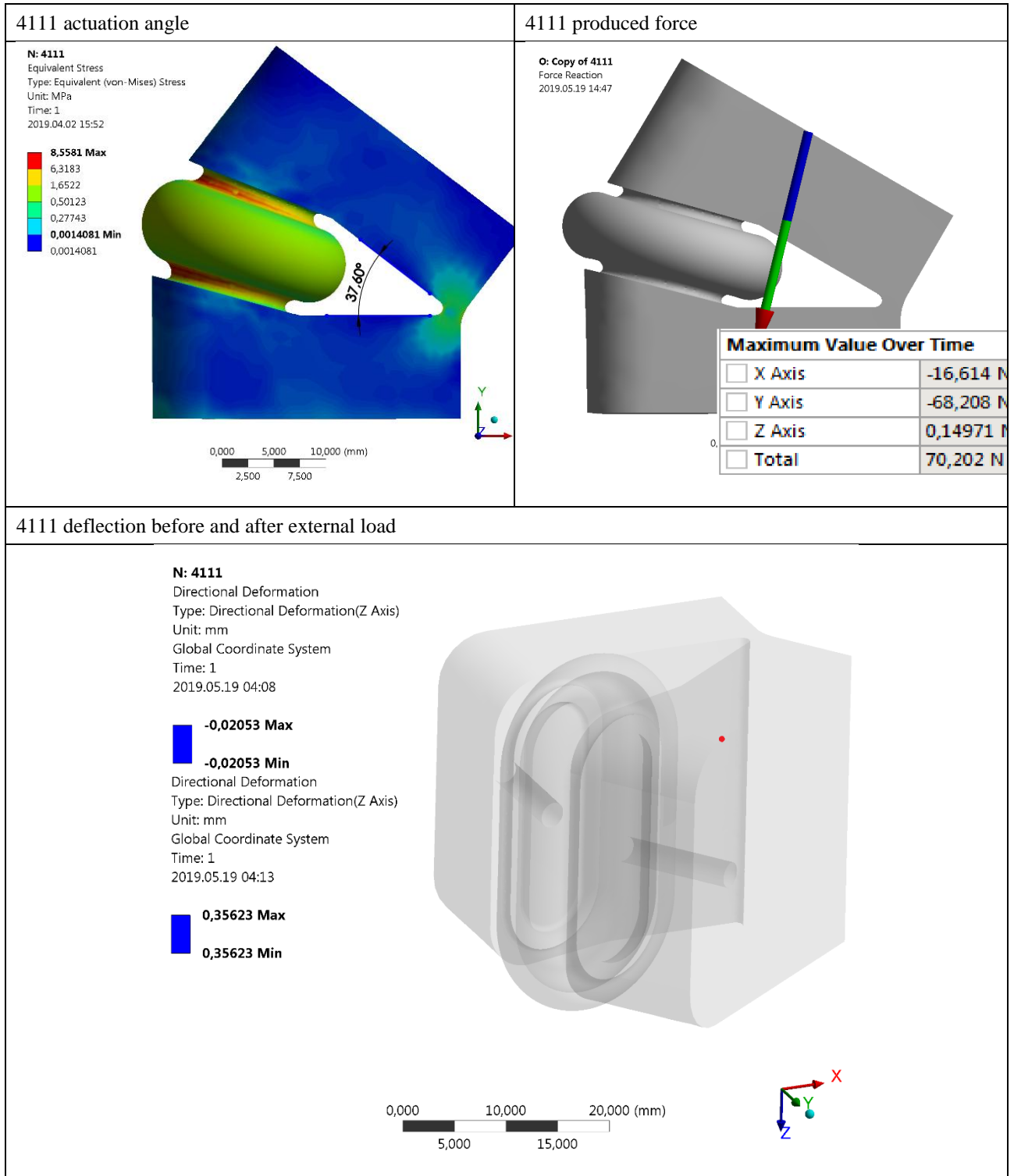
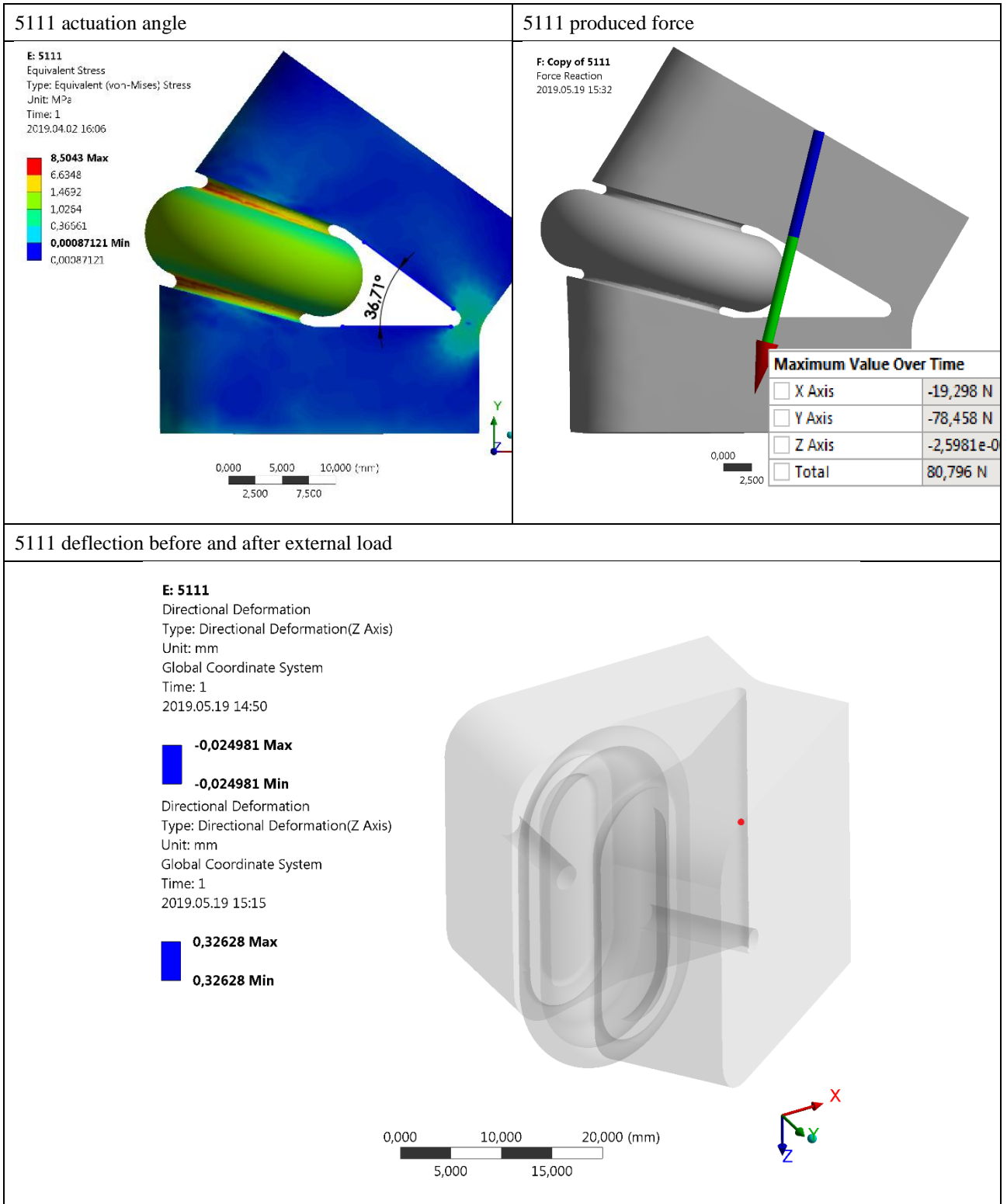


**Table 22.** Variant 5111 results





## Appendix 2. Alteration of pseudo-rigid block area affected by pressure (group 1X11)

### results

**Table 23.** Variant 1211 results

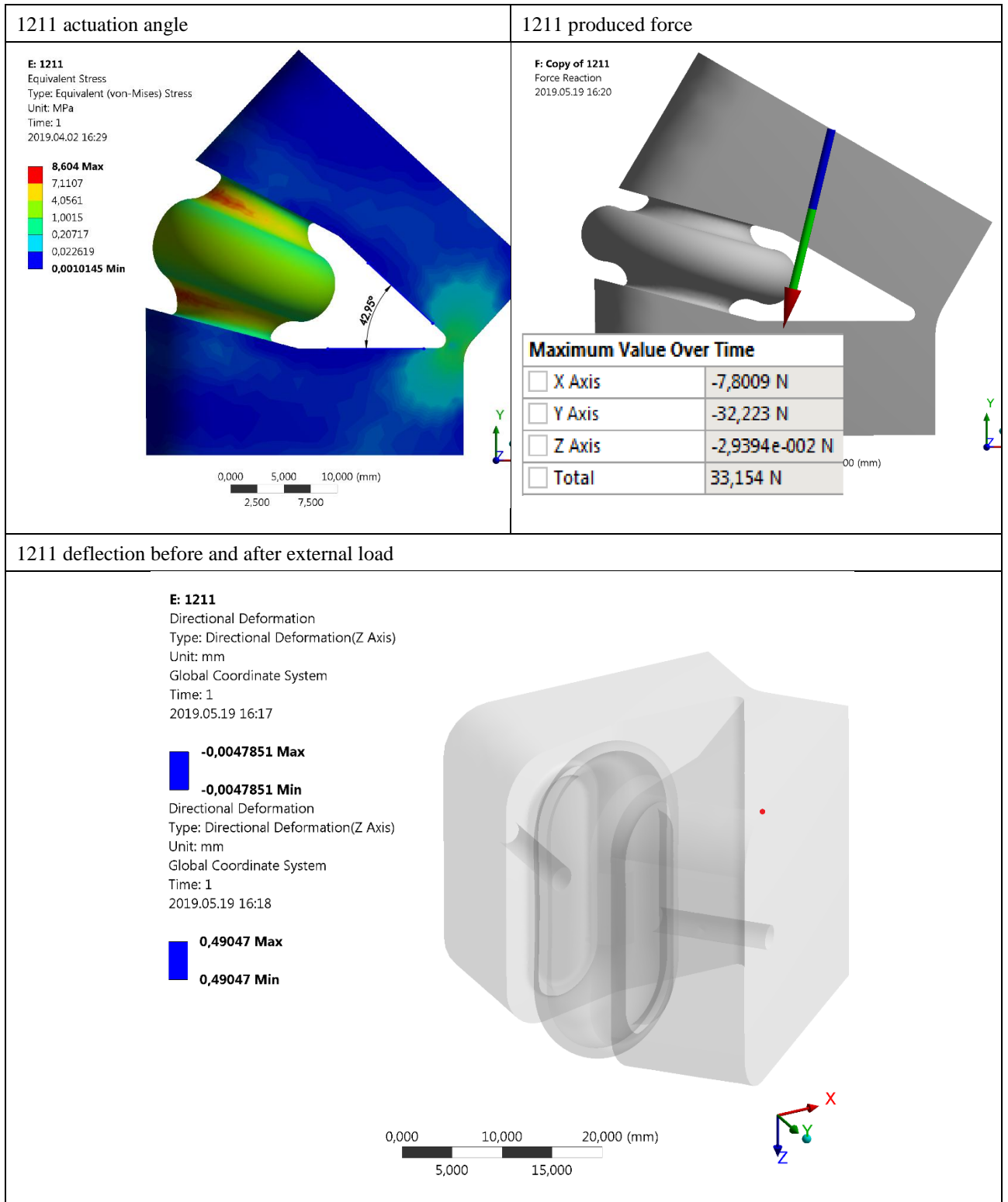


**Table 24.** Variant 1311 results

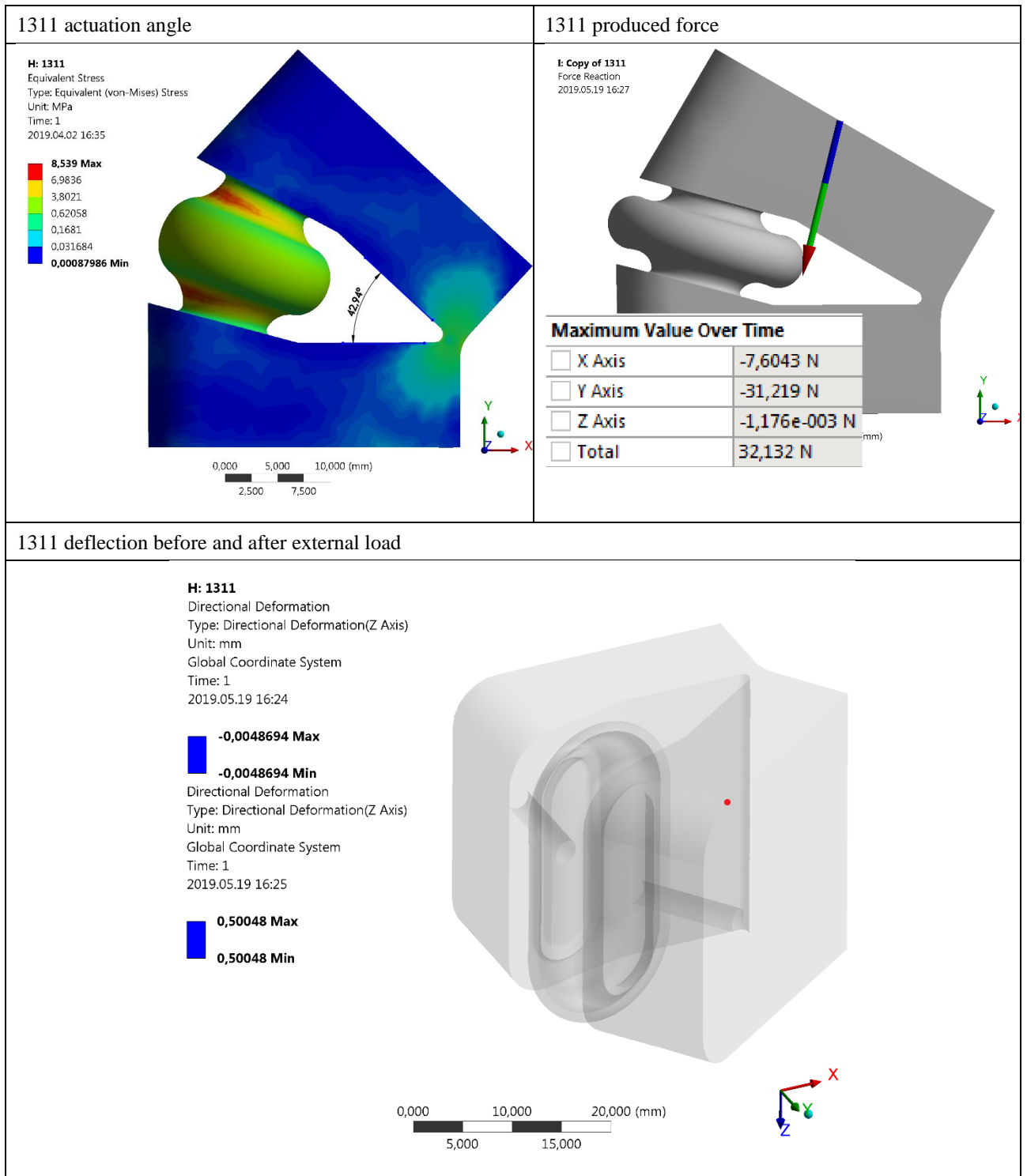


**Table 25.** Variant 1411 results

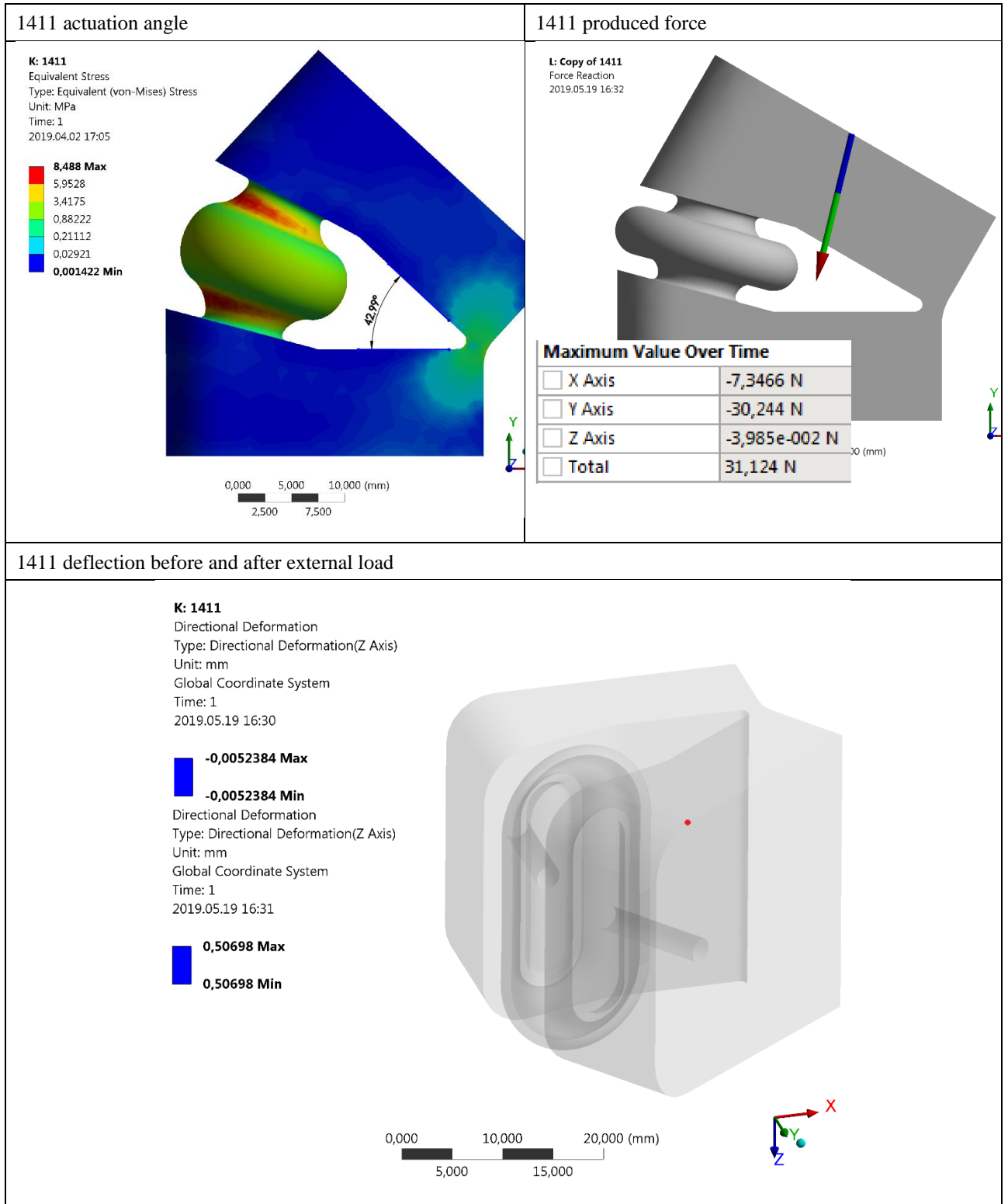
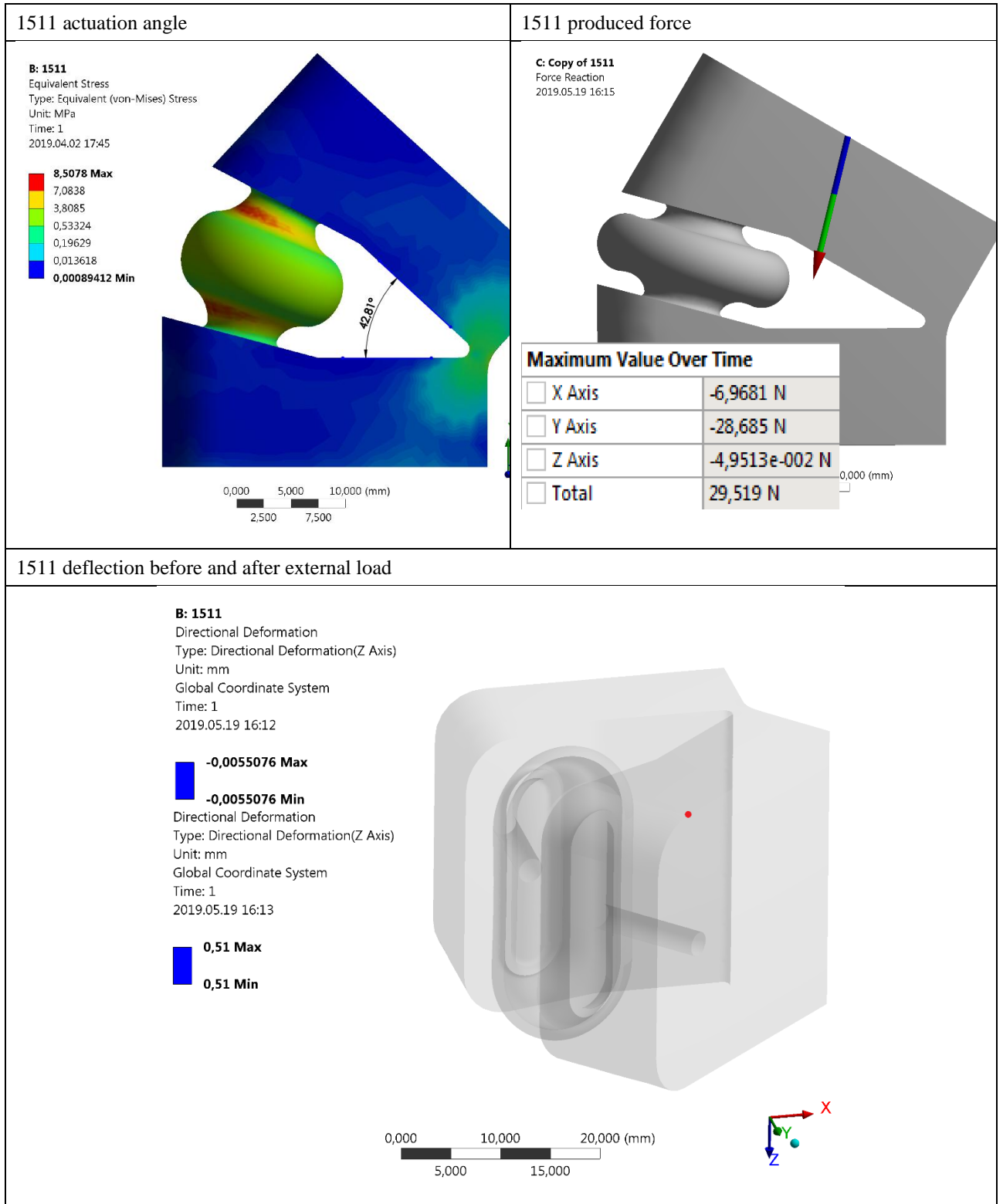


**Table 26.** Variant 1511 results



### Appendix 3. Alteration of compliant element thickness (group 11X1) results

**Table 27.** Variant 1121 results

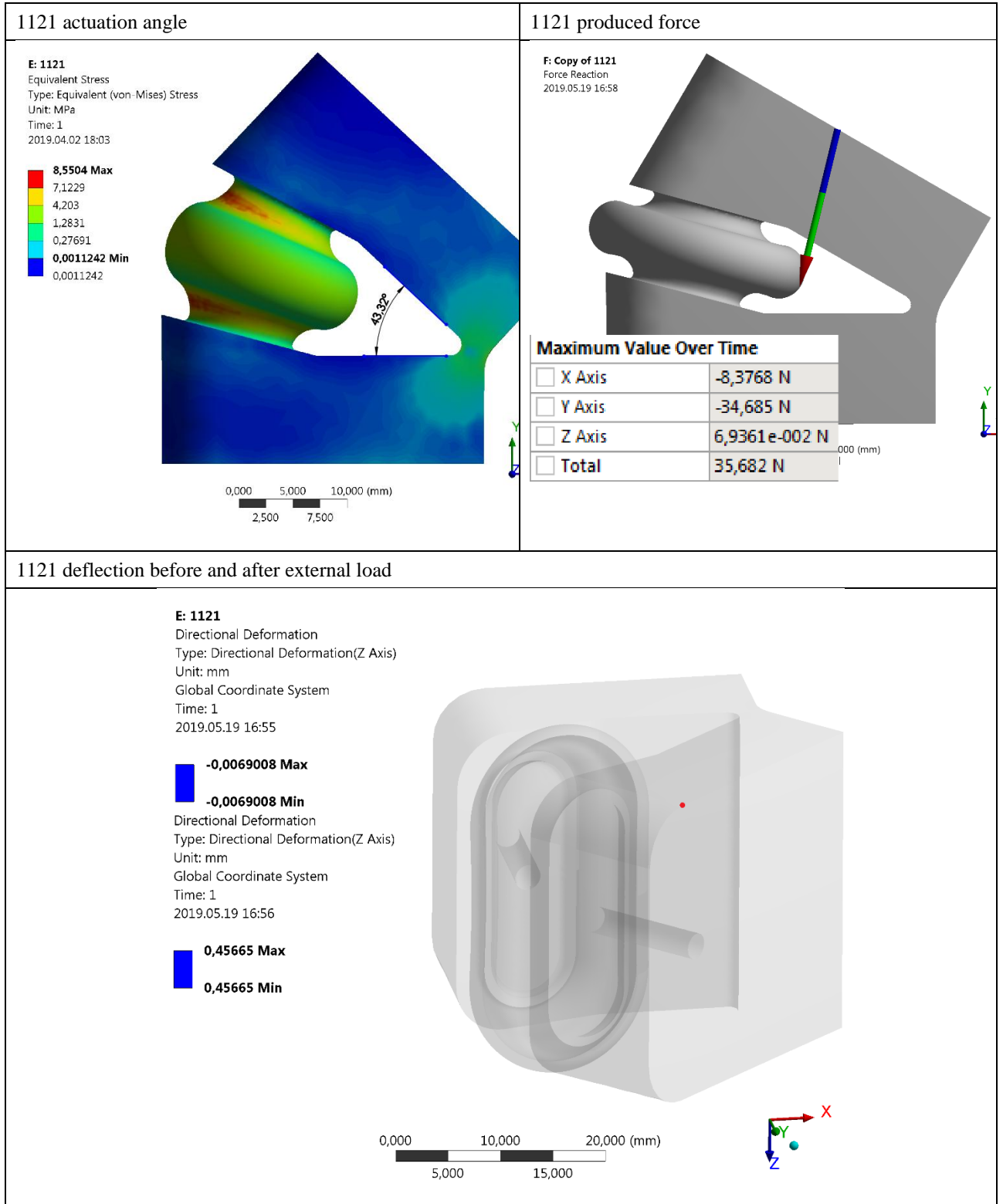


**Table 28.** Variant 1131 results

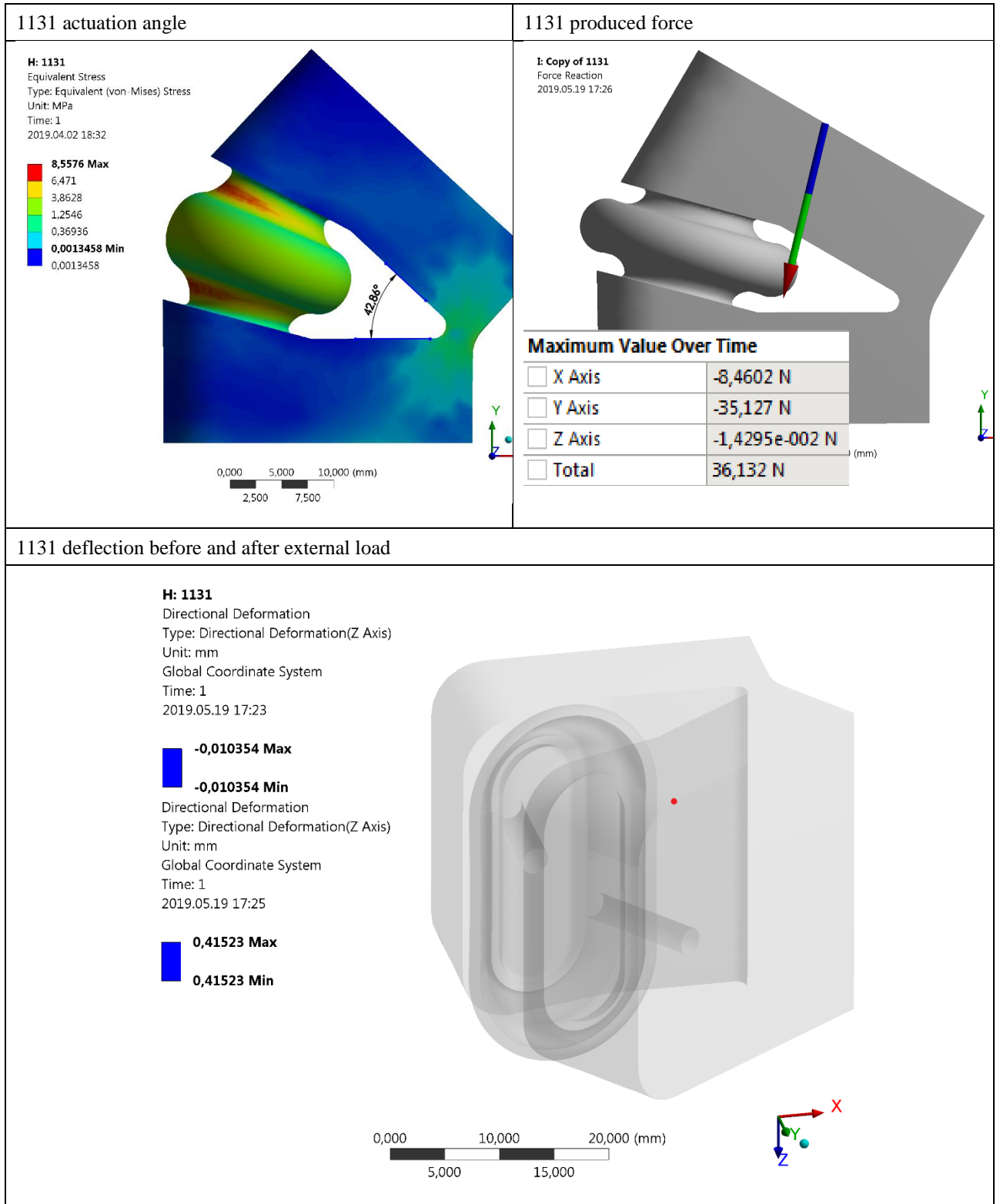


**Table 29.** Variant 1141 results

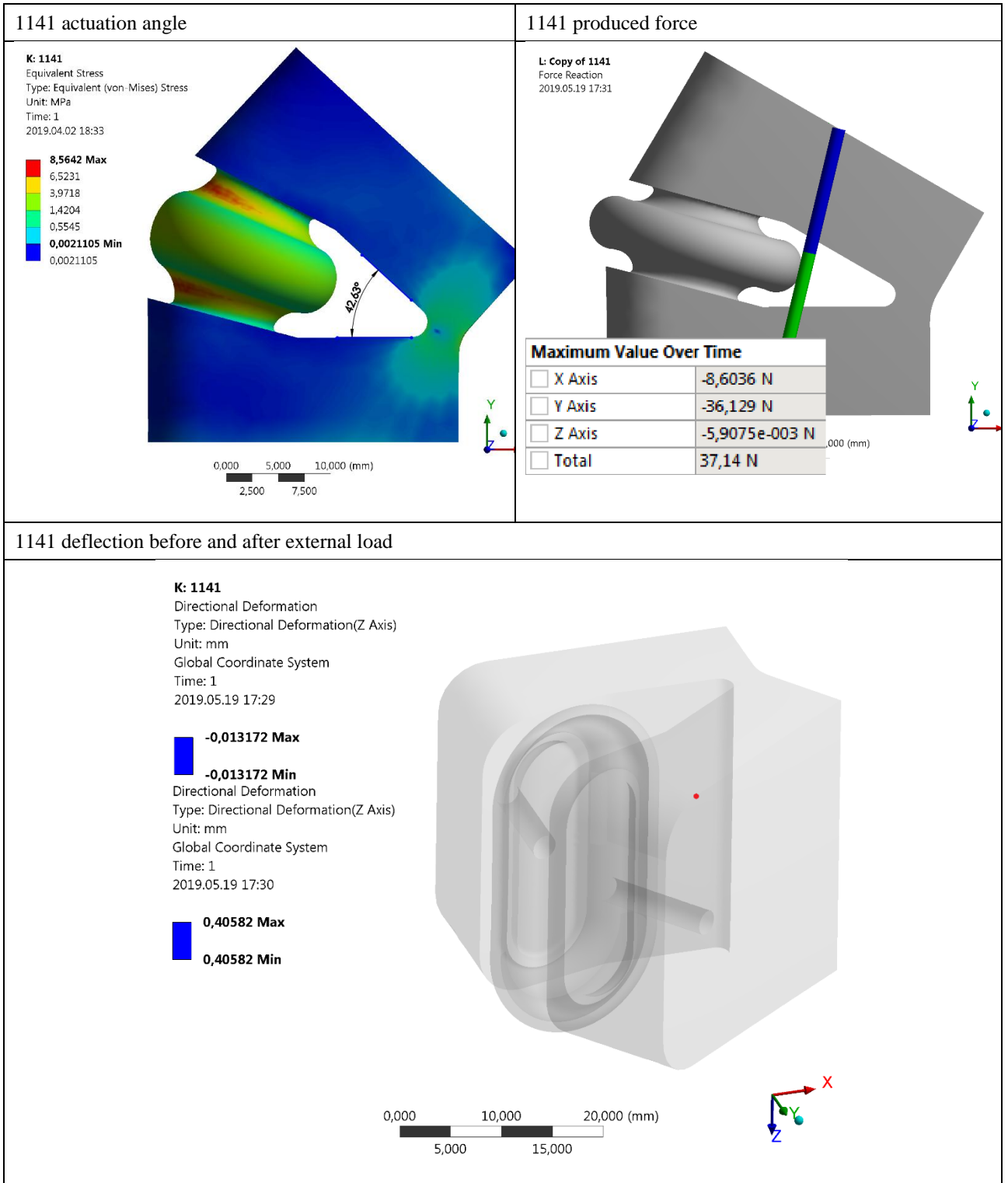
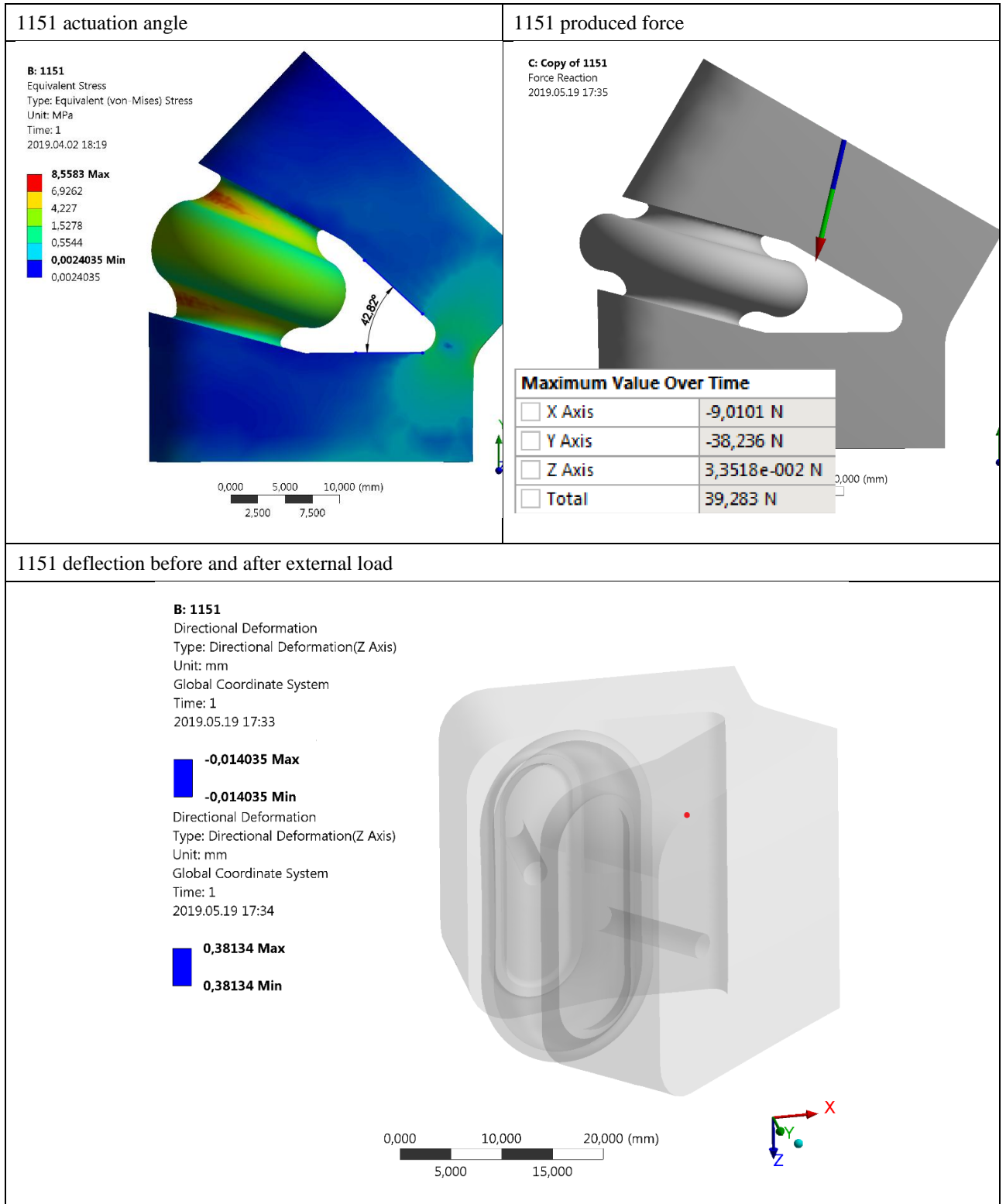


**Table 30.** Variant 1151 results





## Appendix 4. Alteration of inflatable bladder material excess (group 111X) results

**Table 31.** Variant 1112 results

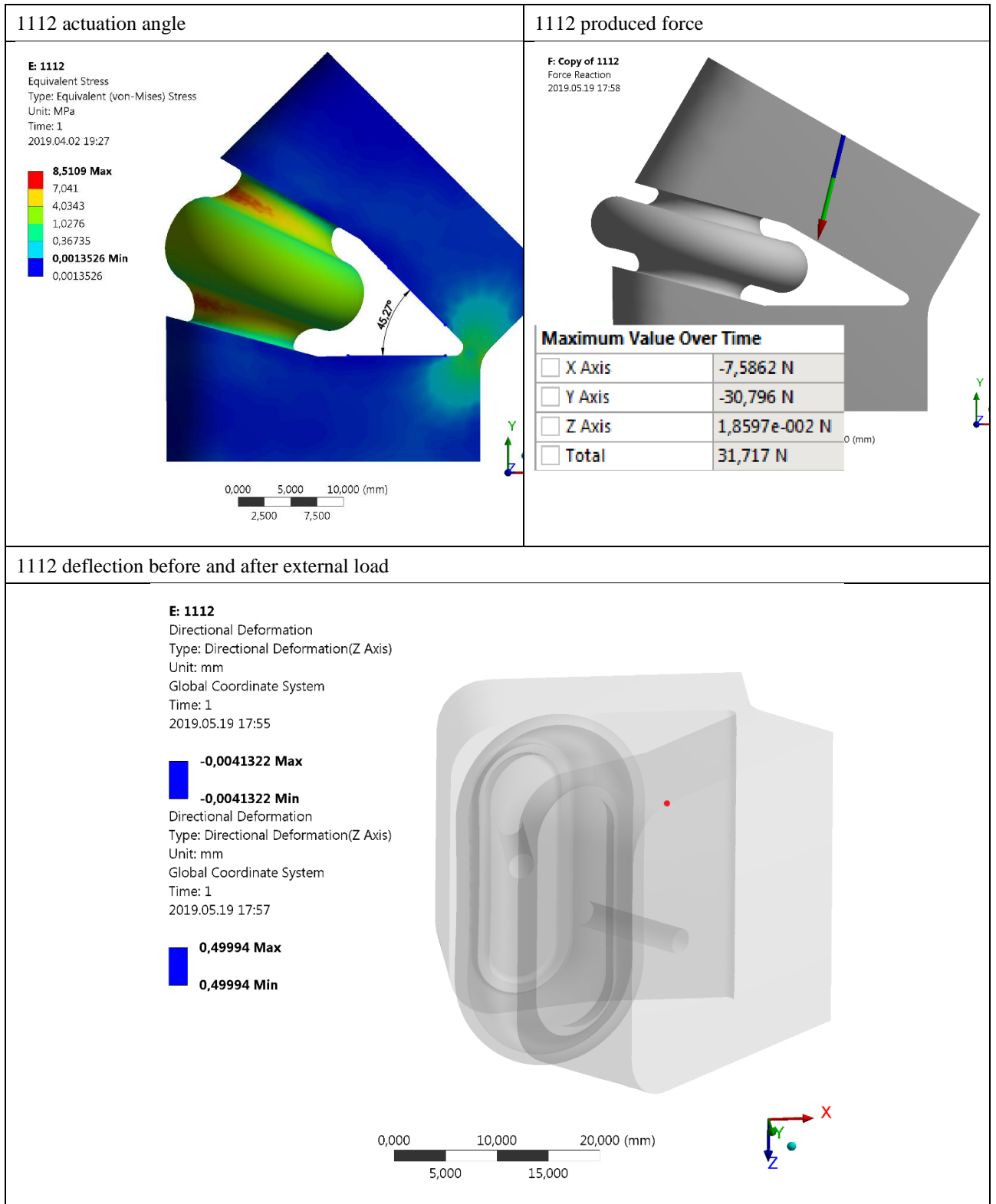


**Table 32.** Variant 1113 results

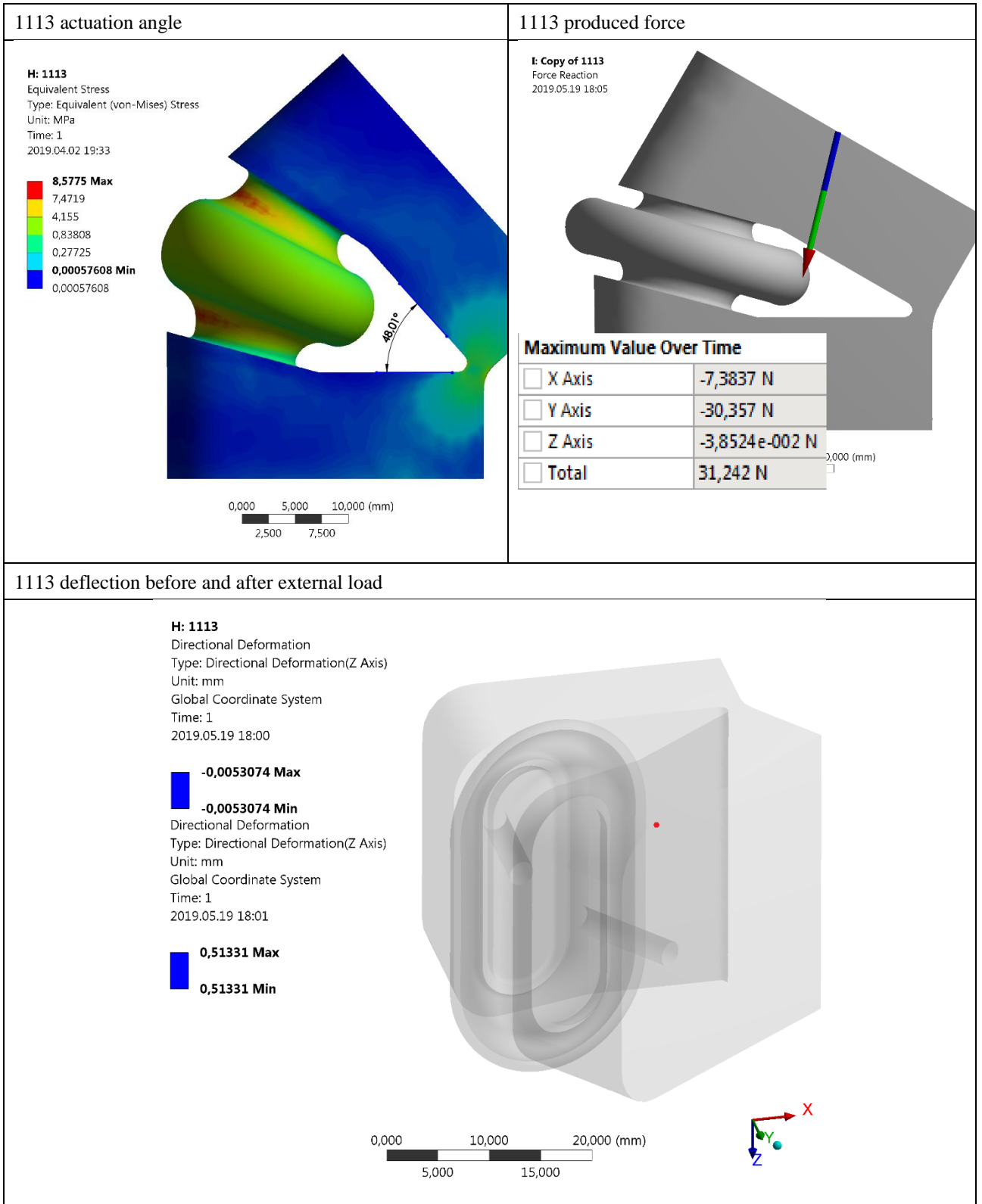


**Table 33.** Variant 1114 results

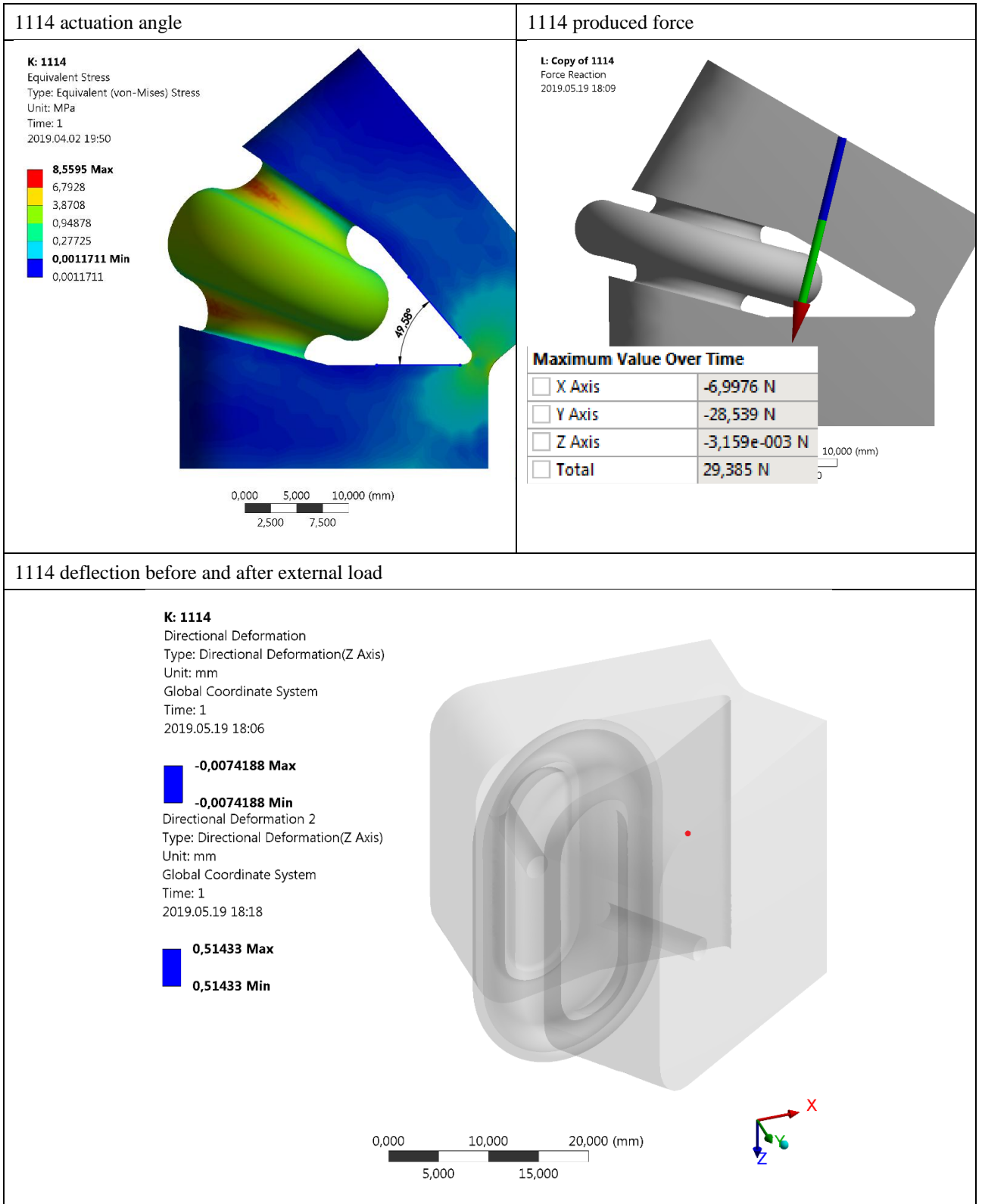


**Table 34.** Variant 1115 results

